

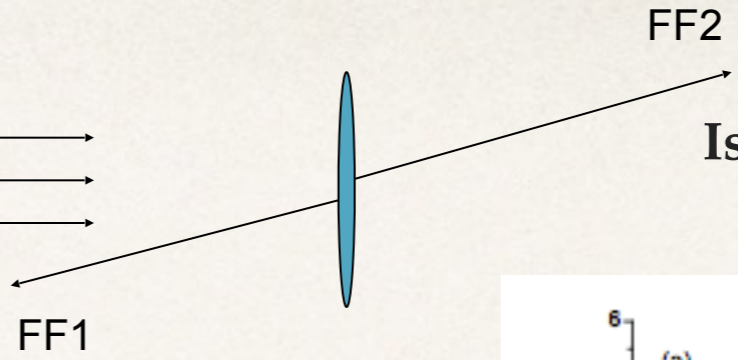
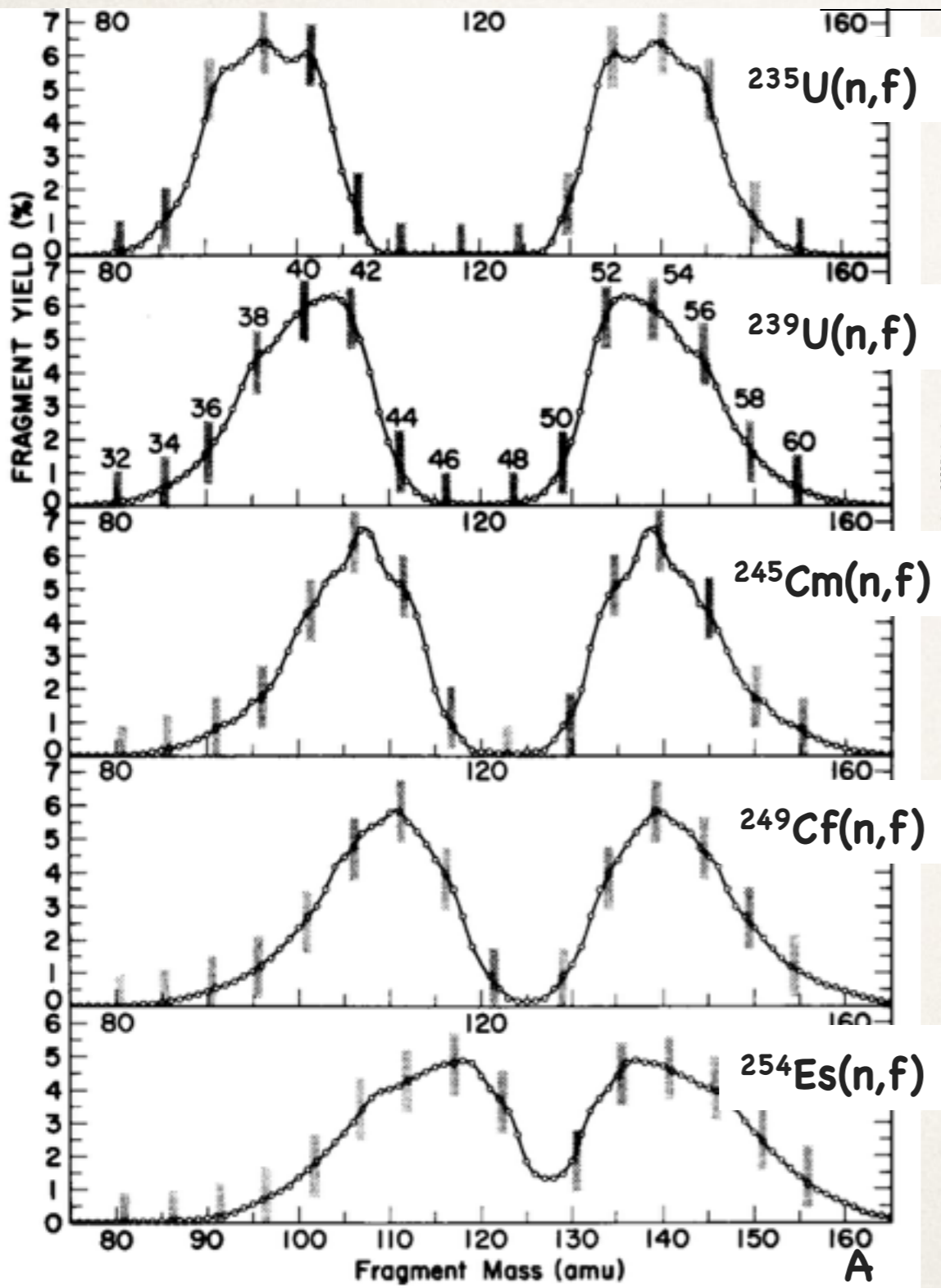
Isotopic Fragment Distribution of Minor Actinides produced in Transfer Reactions

D. Ramos¹, C. Rodríguez-Tajes², M. Caamaño¹, F. Farget², L. Audouin³, J. Benlliure¹, E. Casarejos⁴, E. Clement², D. Cortina¹, O. Delaune², X. Derkx^{5,*}, A. Dijon², D. Doré⁶, B. Fernández-Domínguez¹, G. de France², A. Heinz⁷, B. Jacquot², A. Navin², C. Paradela¹, M. Rejmund², T. Roger², M.-D. Salsac⁶, C. Schmitt²

(1) GENP, Dpto. Física de Partículas, USC, Santiago de Compostela, Spain. (2) GANIL, CEA/DMS - CNRS/IN2P3, Caen, France. (3) IPN Orsay, Université de Paris-Sud XI - CNRS/IN2P3, Orsay, France. (4) CIMA, Escuela Técnica Superior de Ingenieros Industriales, UVigo, Vigo, Spain. (5) LPC Caen, Université de Caen Basse-Normandie – ENSICAEN - CNRS/IN2P3, Caen, France. (6) CEA Saclay, DSM/IRFU/SPhN, Saclay, France. (7) Chalmers University of Technology, Göteborg, Sweden.

Limitations of Direct Kinematics

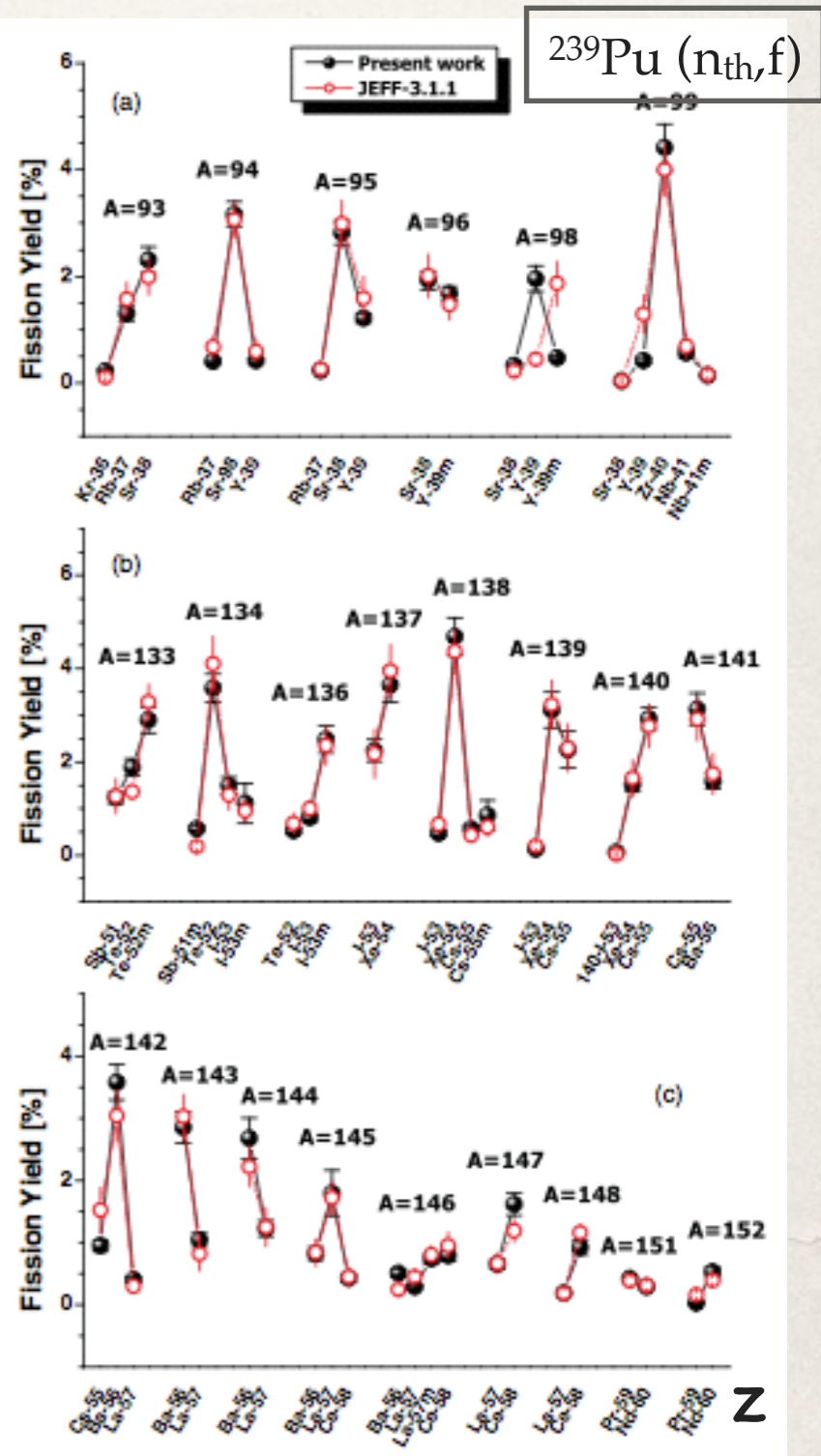
Good measurement of mass distribution



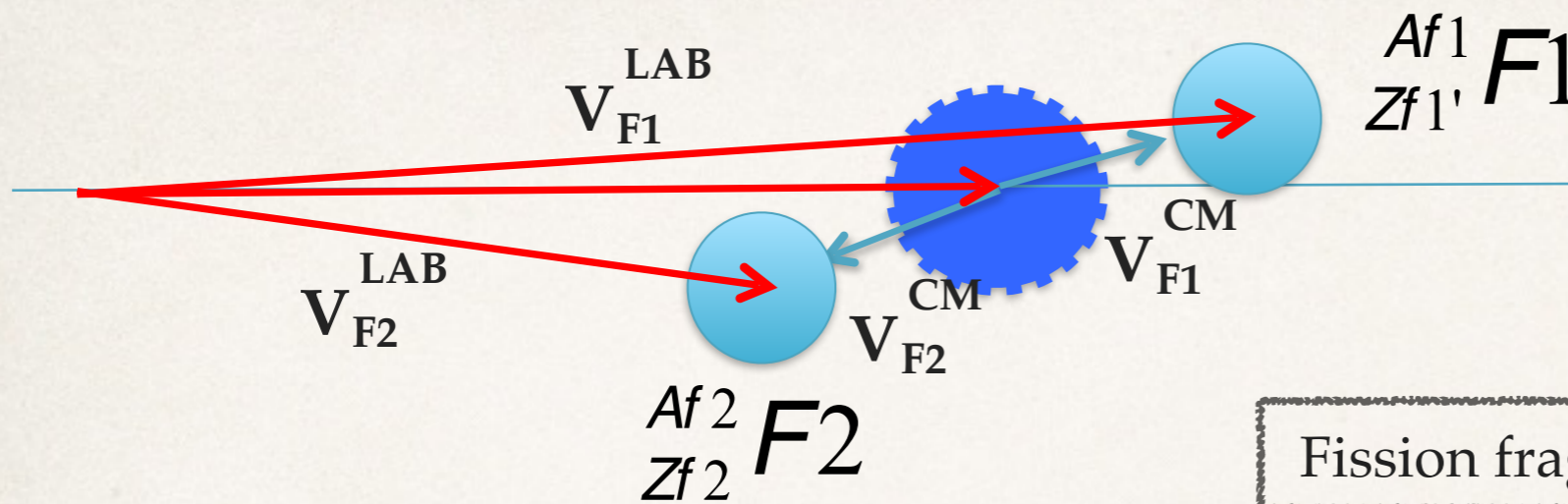
Isotopic distribution by γ -spectroscopy

Incomplete Measurements of Isotopic distributions

limitations for heavy ff
- lifetimes
- unknown level schemes



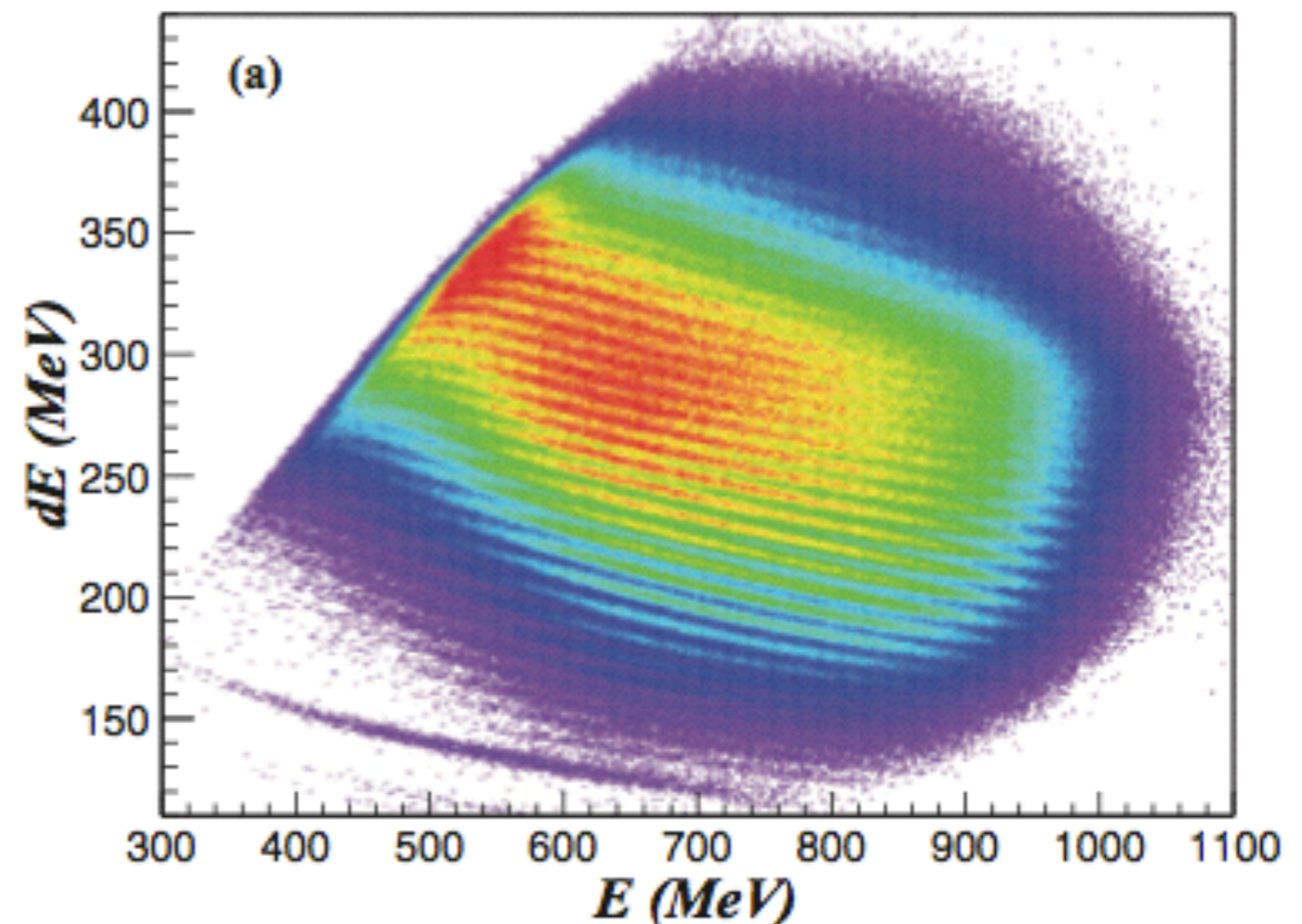
Goals of Inverse kinematics



Fission fragment Z matrix identification

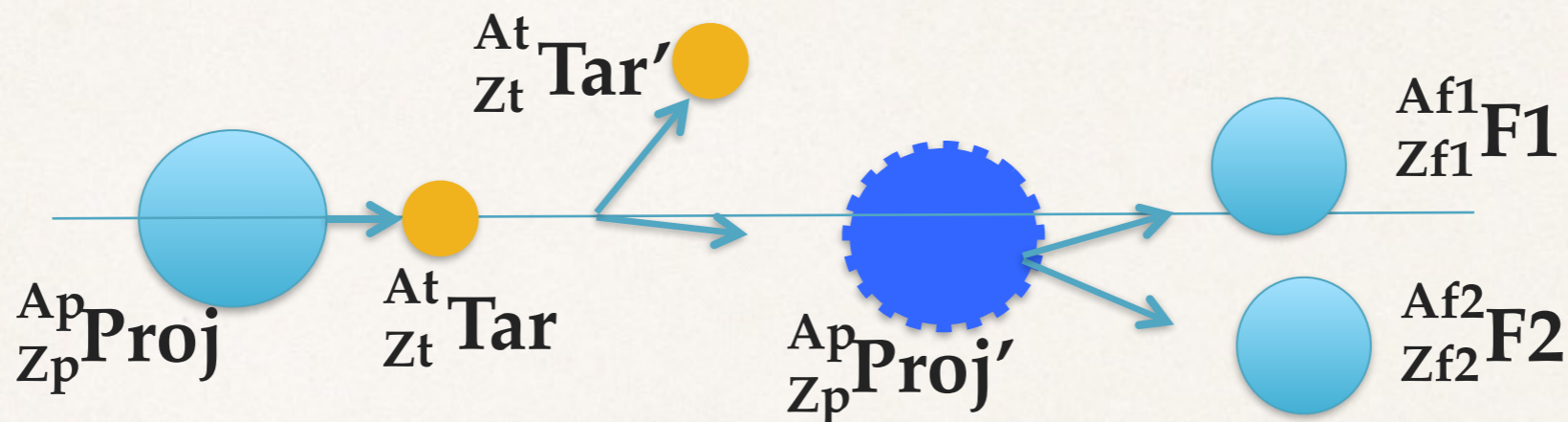
Kinematical boost increases the kinetic energy of the fission fragments providing the capability of a direct identification

Kinematical boost allows to keep a wide angular coverage in the CM frame when the size of the detectors is limited



M. Caamaño et al. PRC 024605 (2013)

Reaction Mechanism



Fissioning Systems

242 Cf	243 Cf	244 Cf	245 Cf	246 Cf	247 Cf	248 Cf	249 Cf	250 Cf	251 Cf	252 Cf
241 Bk	242 Bk	243 Bk	244 Bk	245 Bk	246 Bk	247 Bk	248 Bk	249 Bk	250 Bk	251 Bk
240 Cm	241 Cm	242 Cm	243 Cm	244 Cm	245 Cm	246 Cm	247 Cm	248 Cm	249 Cm	250 Cm
239 Am	240 Am	241 Am	242 Am	243 Am	244 Am	245 Am	246 Am	247 Am	248 Am	249 Am
238 Pu	239 Pu	240 Pu	241 Pu	242 Pu	243 Pu	244 Pu	245 Pu	246 Pu	247 Pu	
237 Np	238 Np	239 Np	240 Np	241 Np	242 Np	243 Np	244 Np			
236 U	237 U	238 U	239 U	240 U	241 U	242 U				

Fissioning systems not accessible from any other mechanism

10% above Coulomb barrier

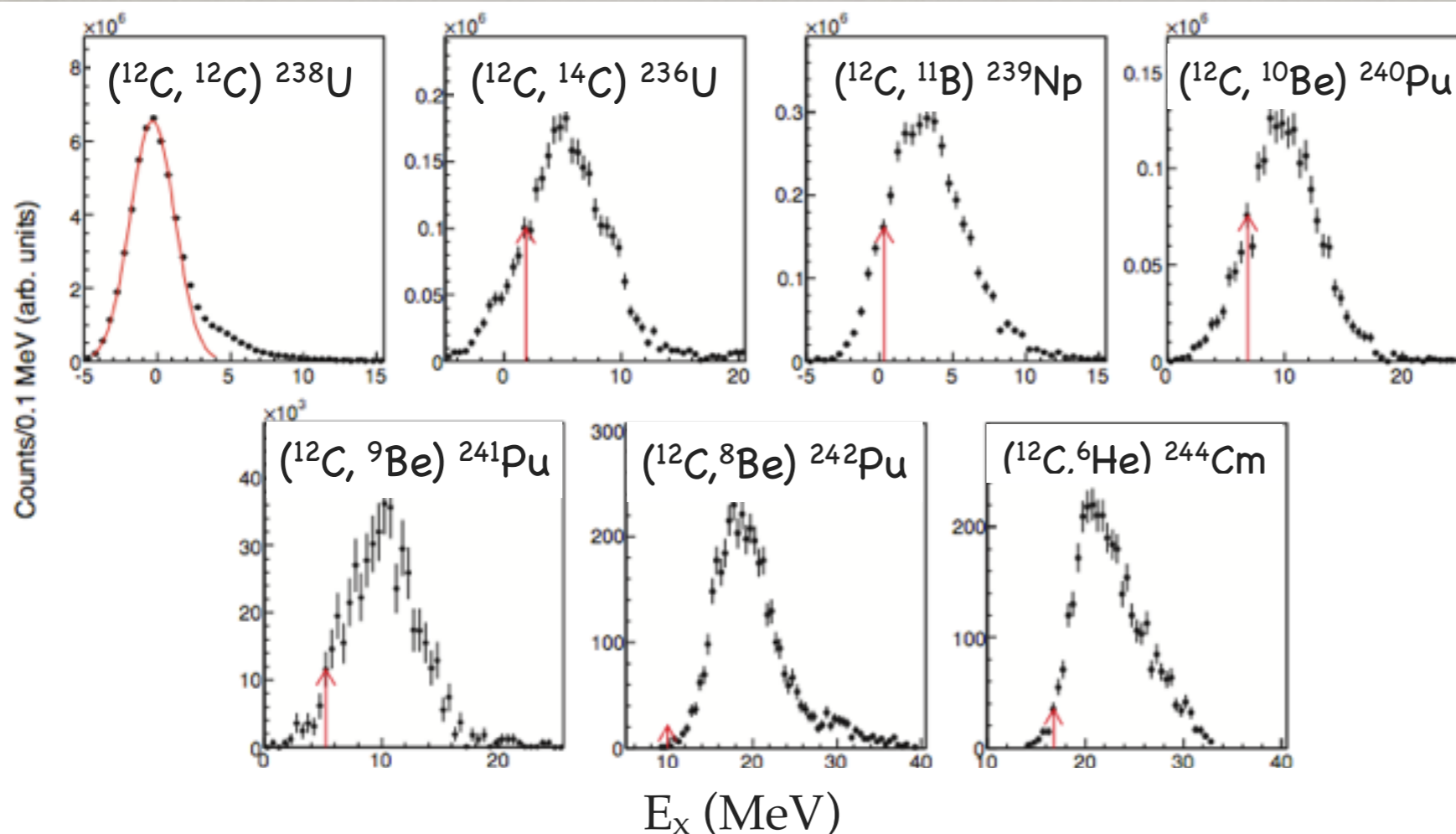
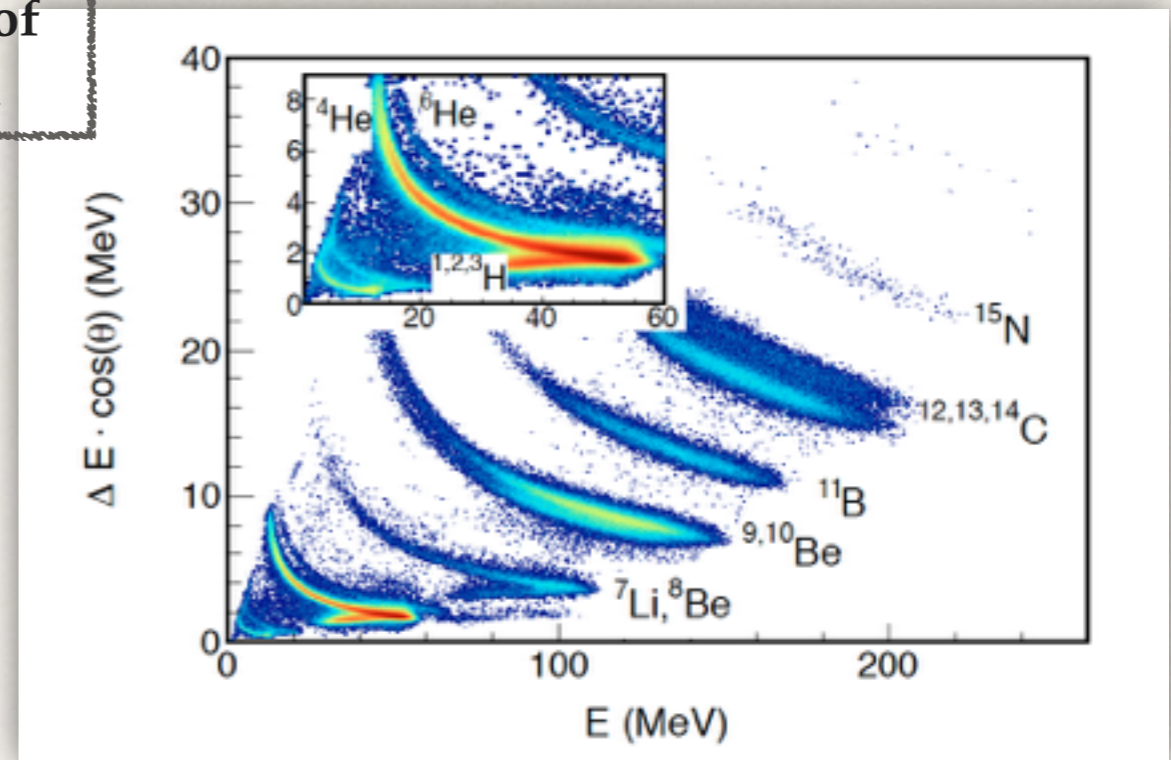
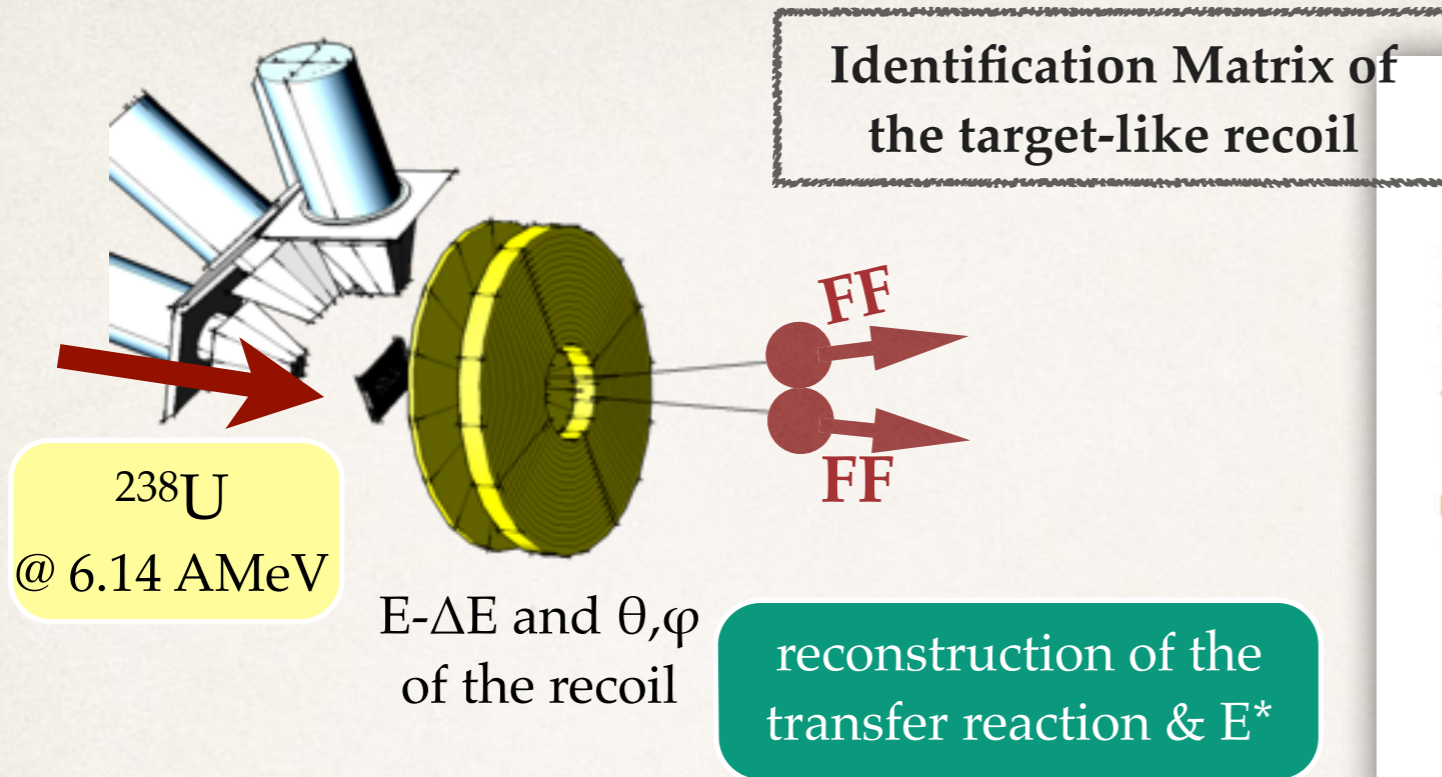
Transfer-Fission:

10 n-rich actinides produced with a distribution of E_x below 30 MeV

Fusion-Fission:

production of ^{250}Cf with $E_x = 45 \text{ MeV}$
10 times more likely than any transfer channel

Transfer Reaction and Excitation Energy



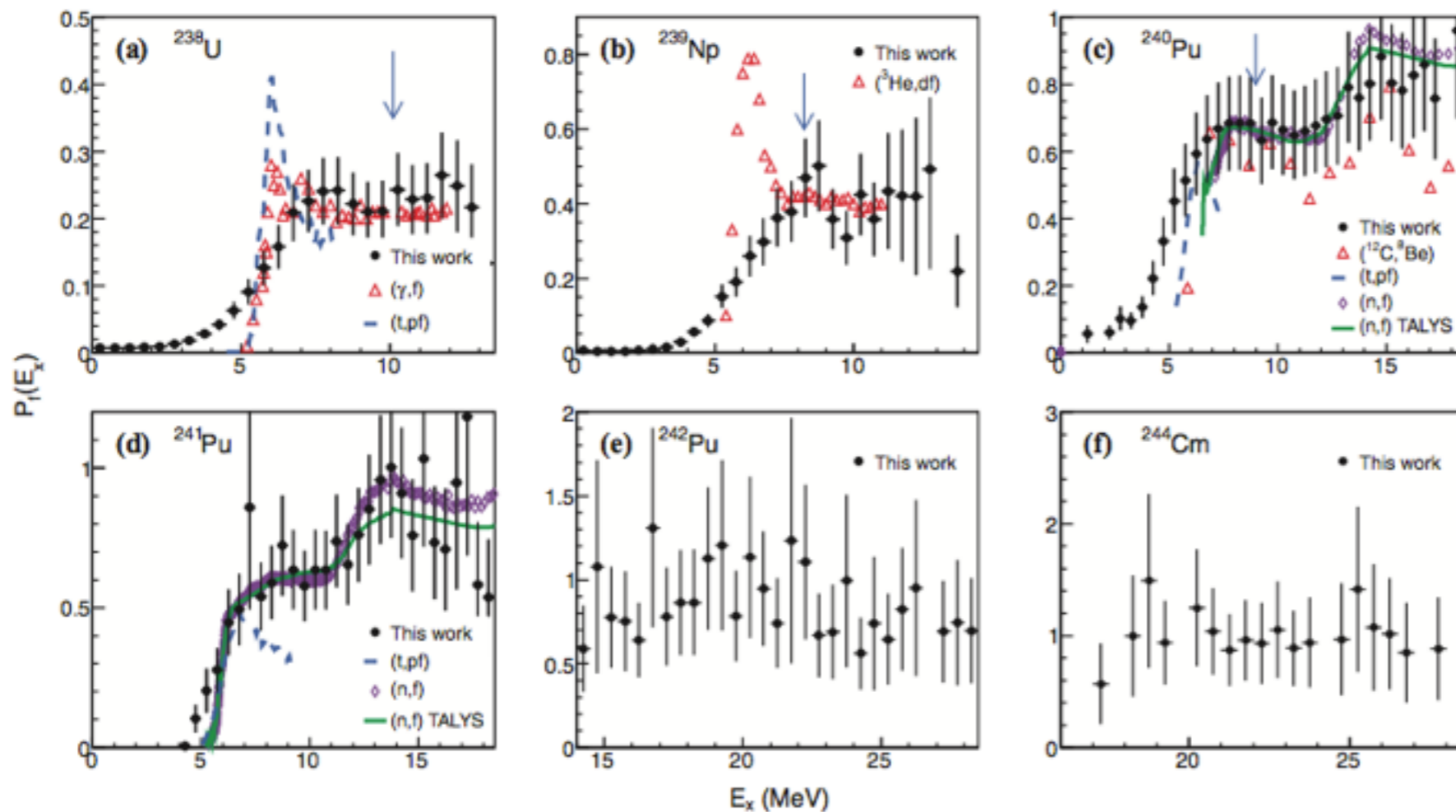
Distribution of E_x for the different fissioning systems from reconstruction of the binary reaction

Higher E_x for higher number of transferred nucleons

$E_x \sim 8$ MeV is comparable with fast-neutron fission

C. Rodriguez-Tajes et al.,
PRC (2014) 024614

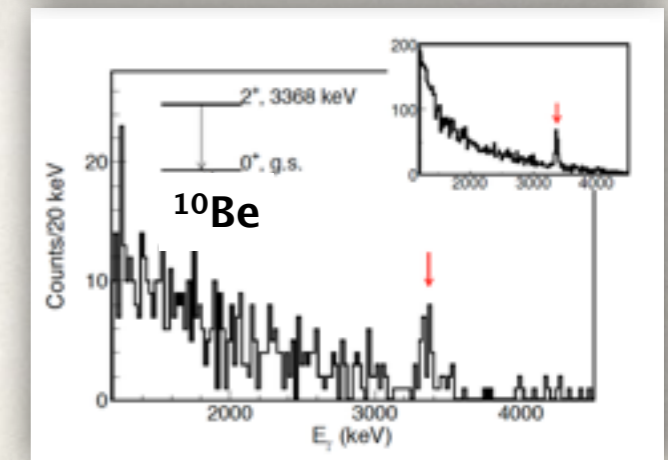
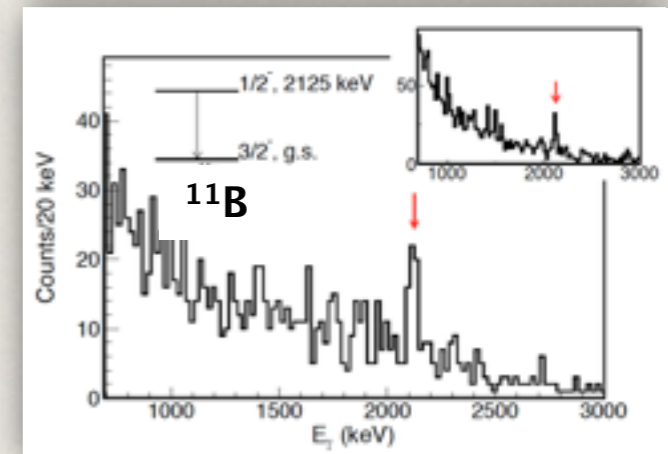
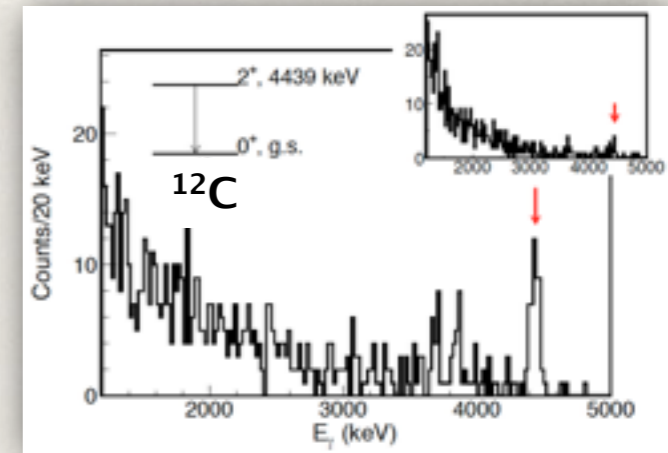
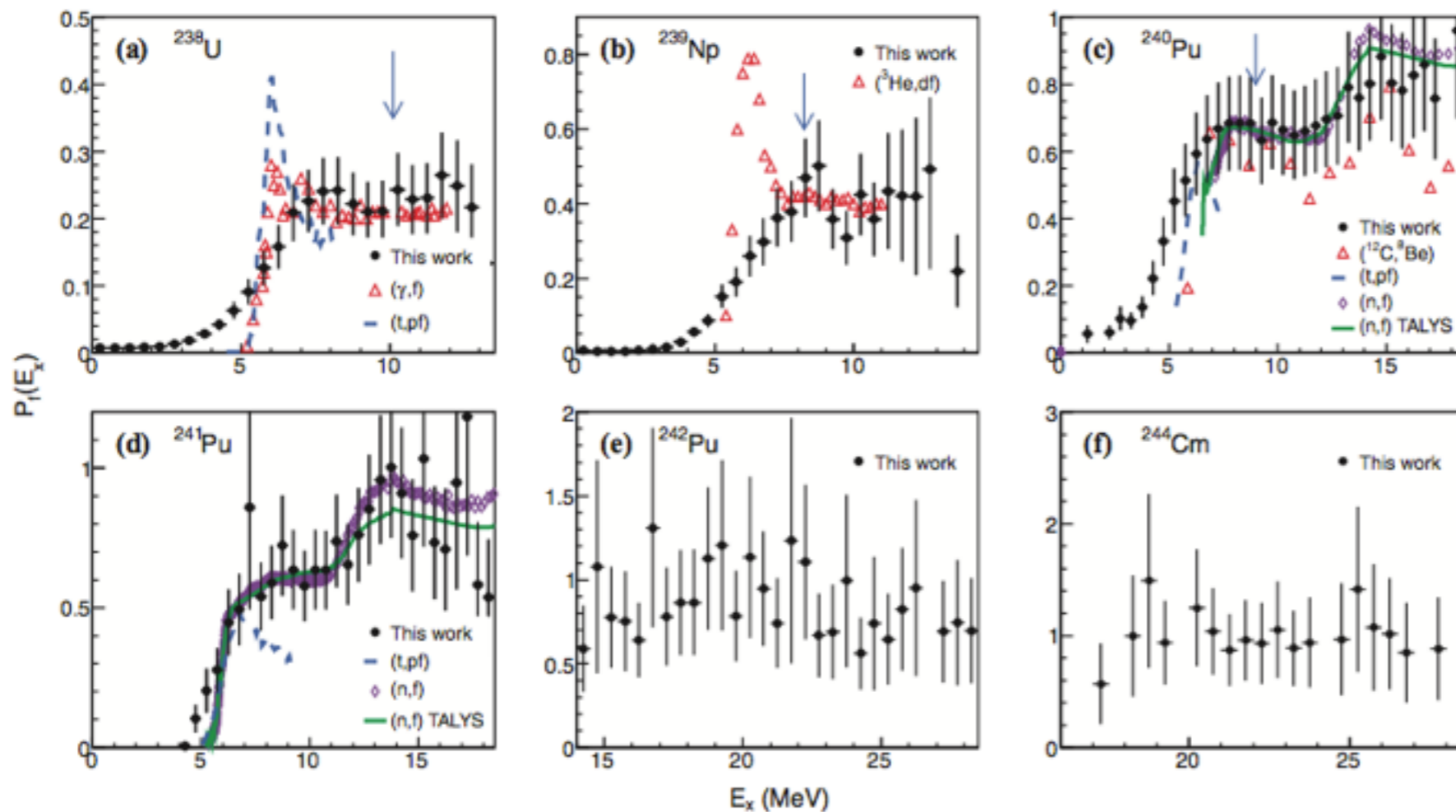
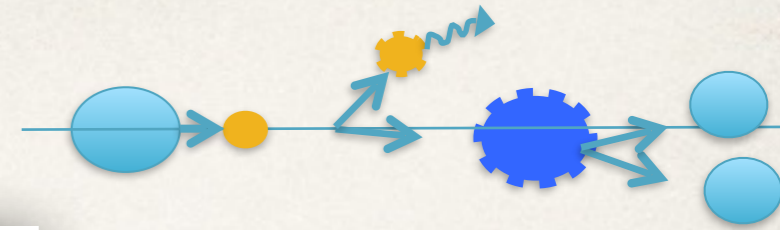
Fission Probabilities & Excitation of Target-like Recoil



We observe a general agreement with previous data with small discrepancies

this experiment provides data never measured before for ^{242}Pu and ^{244}Cm

Fission Probabilities & Excitation of Target-like Recoil

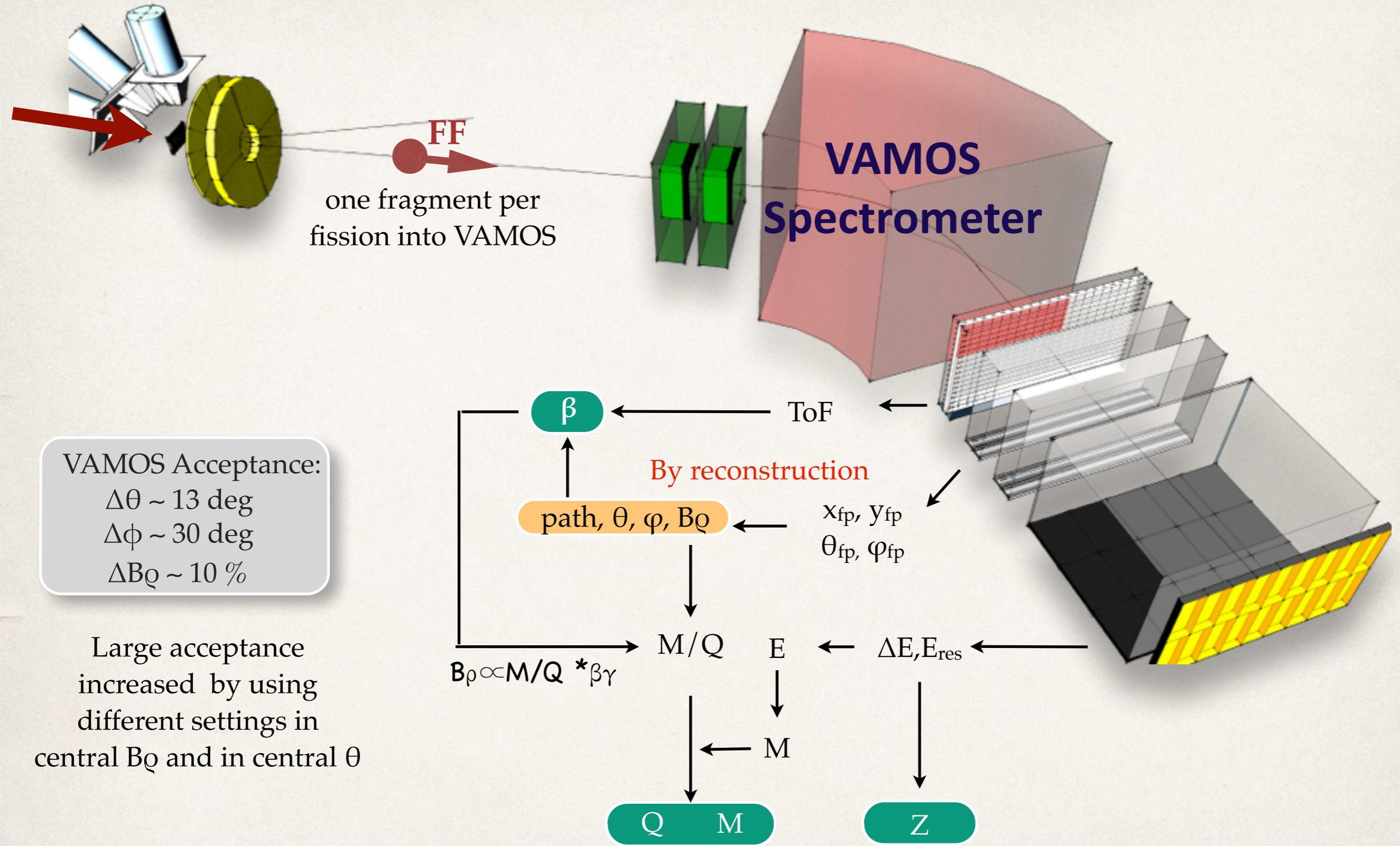


We observe a general agreement with previous data with small discrepancies

this experiment provides data never measured before for ^{242}Pu and ^{244}Cm

γ -rays measurements show excited states in ^{12}C , ^{11}B and ^{10}Be in coincidence with fission with $P_\gamma = 0.12-0.14$

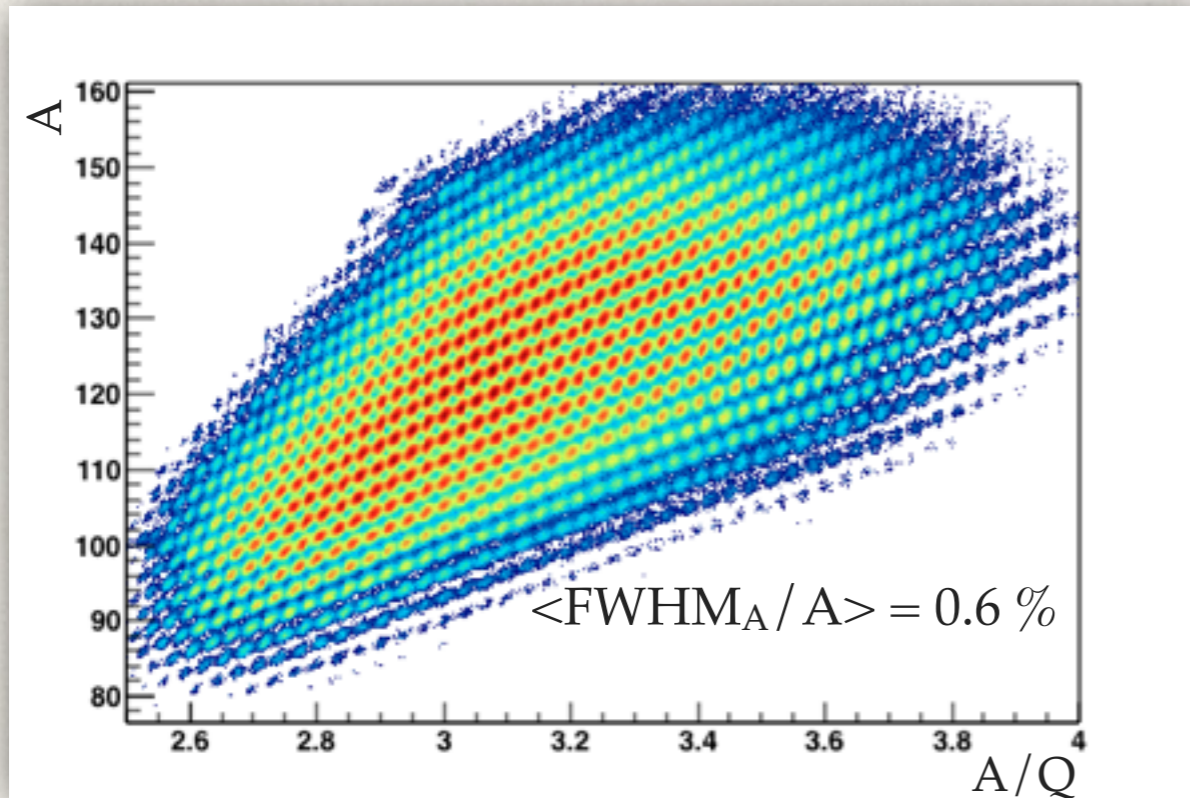
Fission Fragments Detection



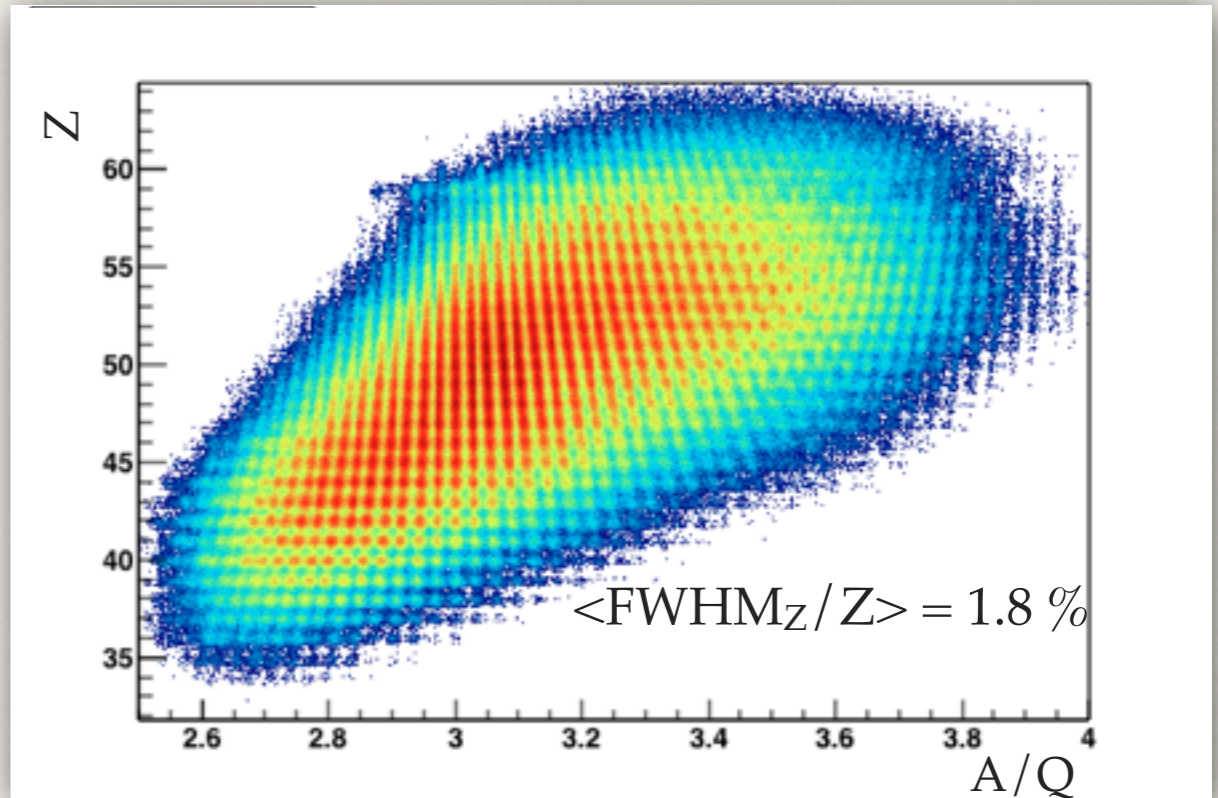
M. Rejmund et al., NIM A 646 (2011) 184
 S. Pullanhiotan et al., NIM A 593 (2008) 343

Fission Fragments Identification

Mass Identification



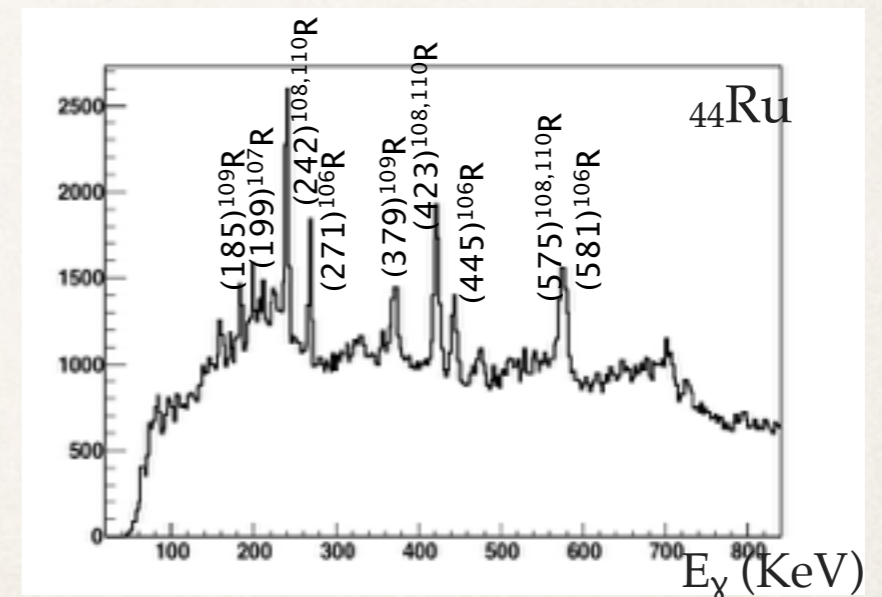
Proton Number Identification



A/Q provides the Q separation and contributes to a better A resolution

More than 300 isotopes identified

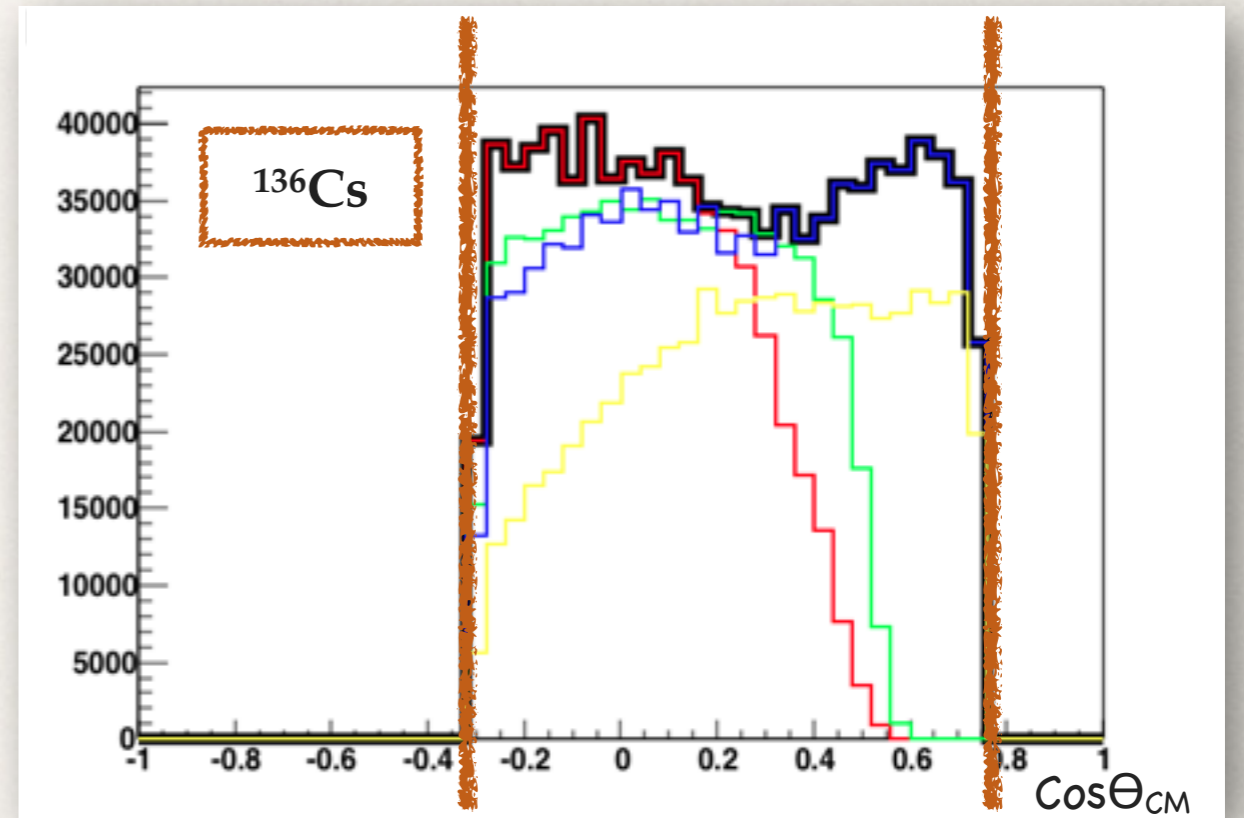
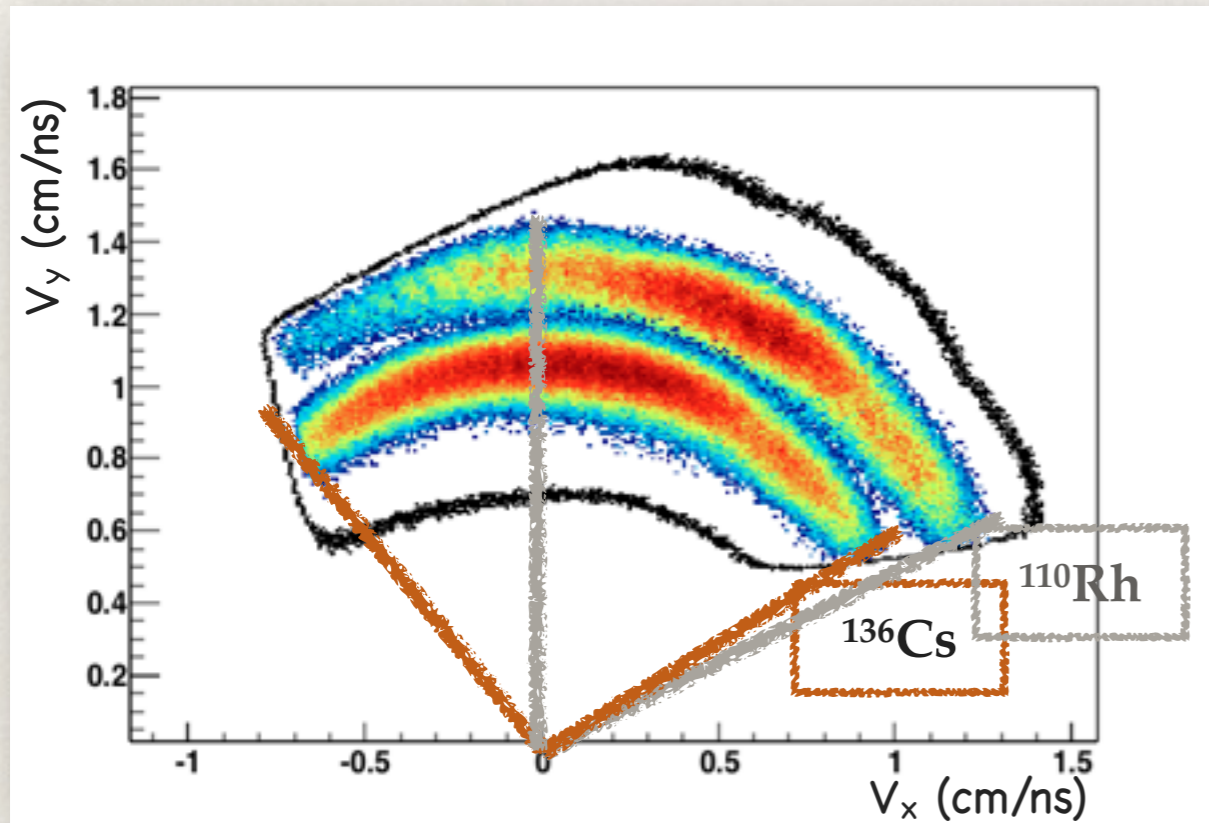
γ -rays in coincidence with fission fragments provide a cross check for the Z and A identification



A. Shrivastava et al. PRC 80 (2009) 051305

Transmission through VAMOS

The detection is limited by the transmission



The transmission is different for different isotopes

$$Y(Z, A) = I(Z, A) \frac{2}{\text{Range}(Z, A)}$$

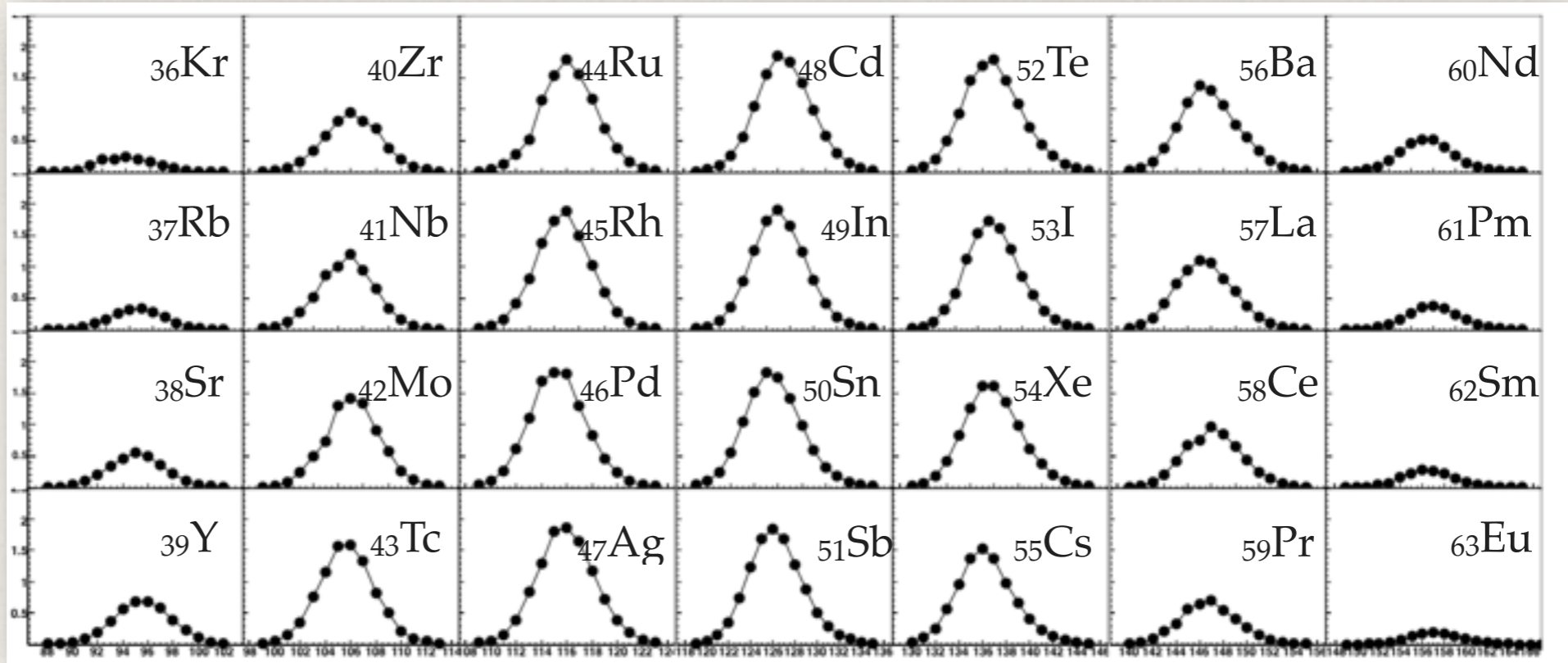
We need to recover all the charge states per isotope and compensate the acceptance in the azimuthal and polar angles

Beam normalization for different settings is required as well

Isotopic Fission Yields

^{250}Cf

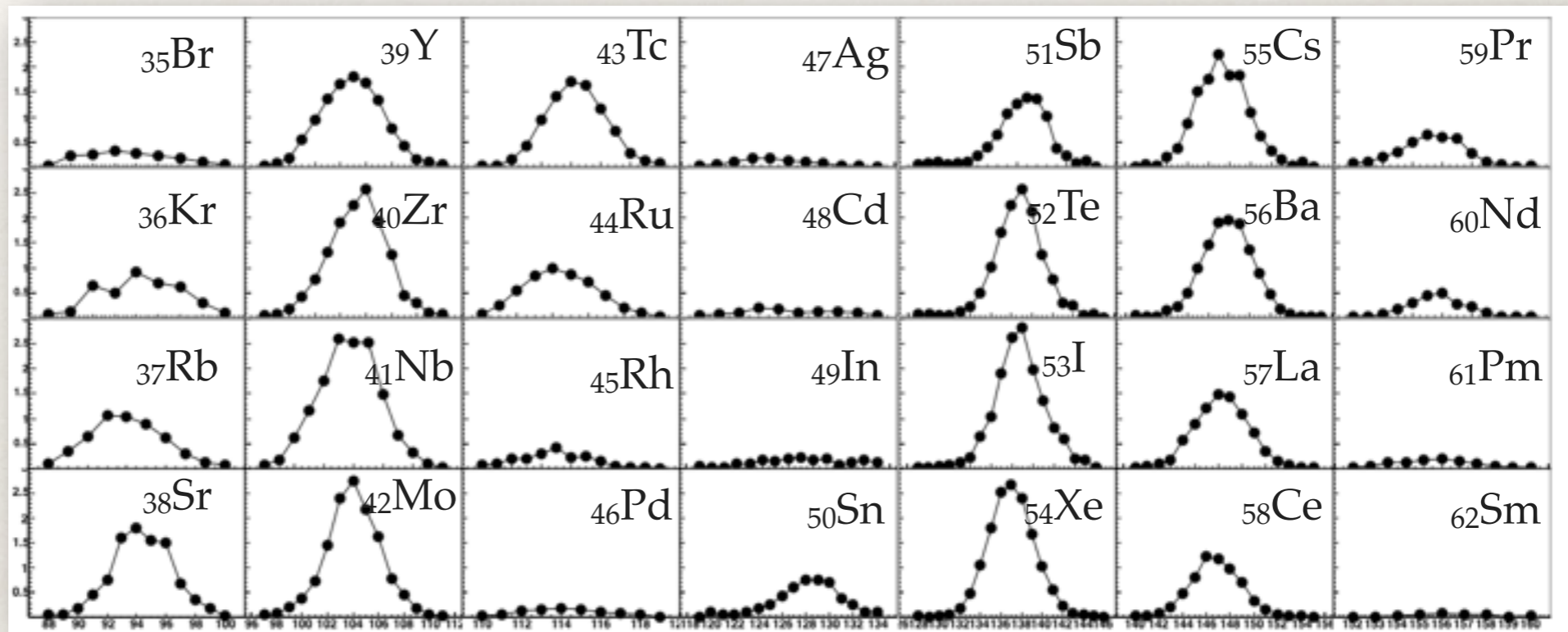
Isotopic Yields in 3 orders of magnitud



A

^{240}Pu

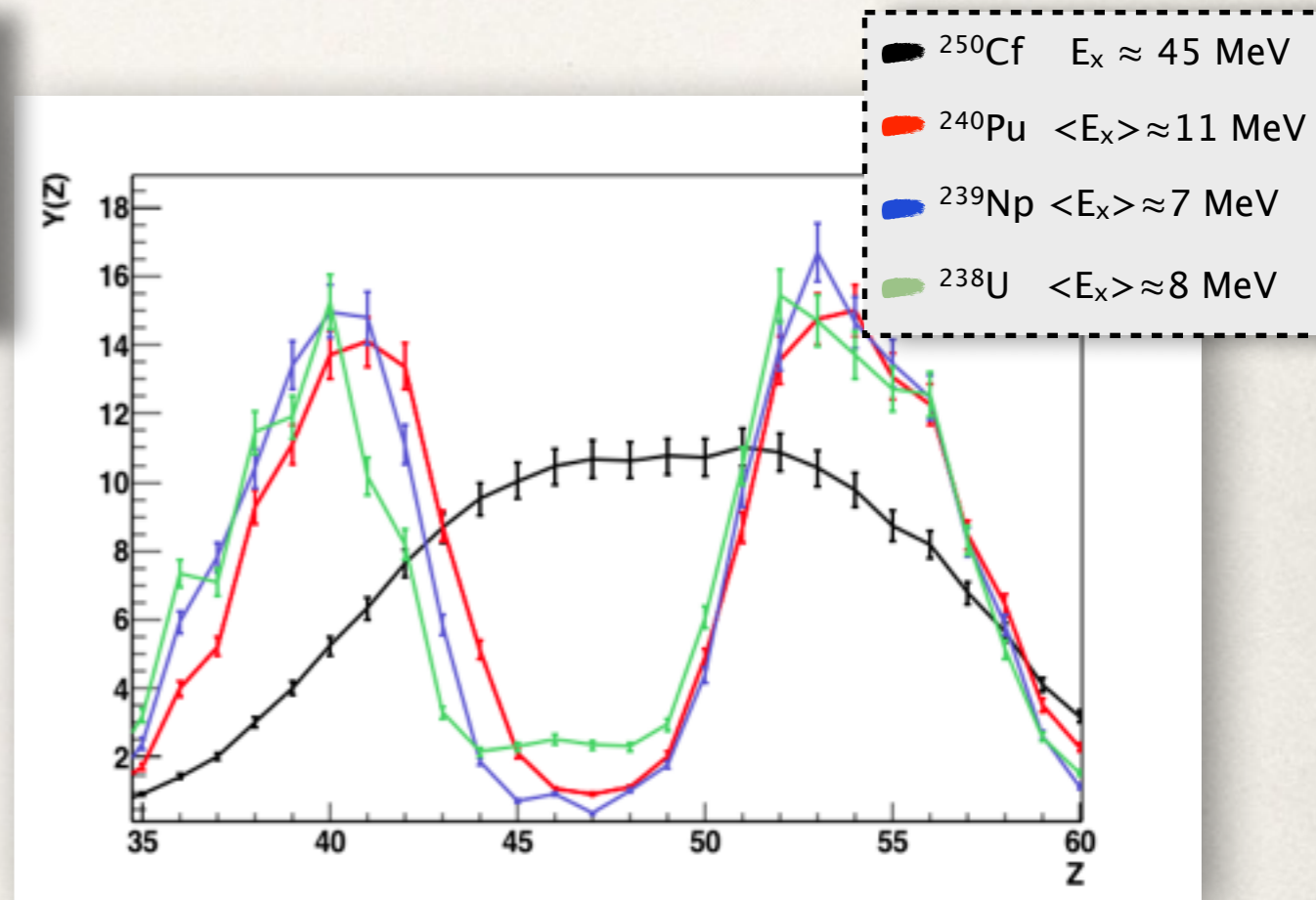
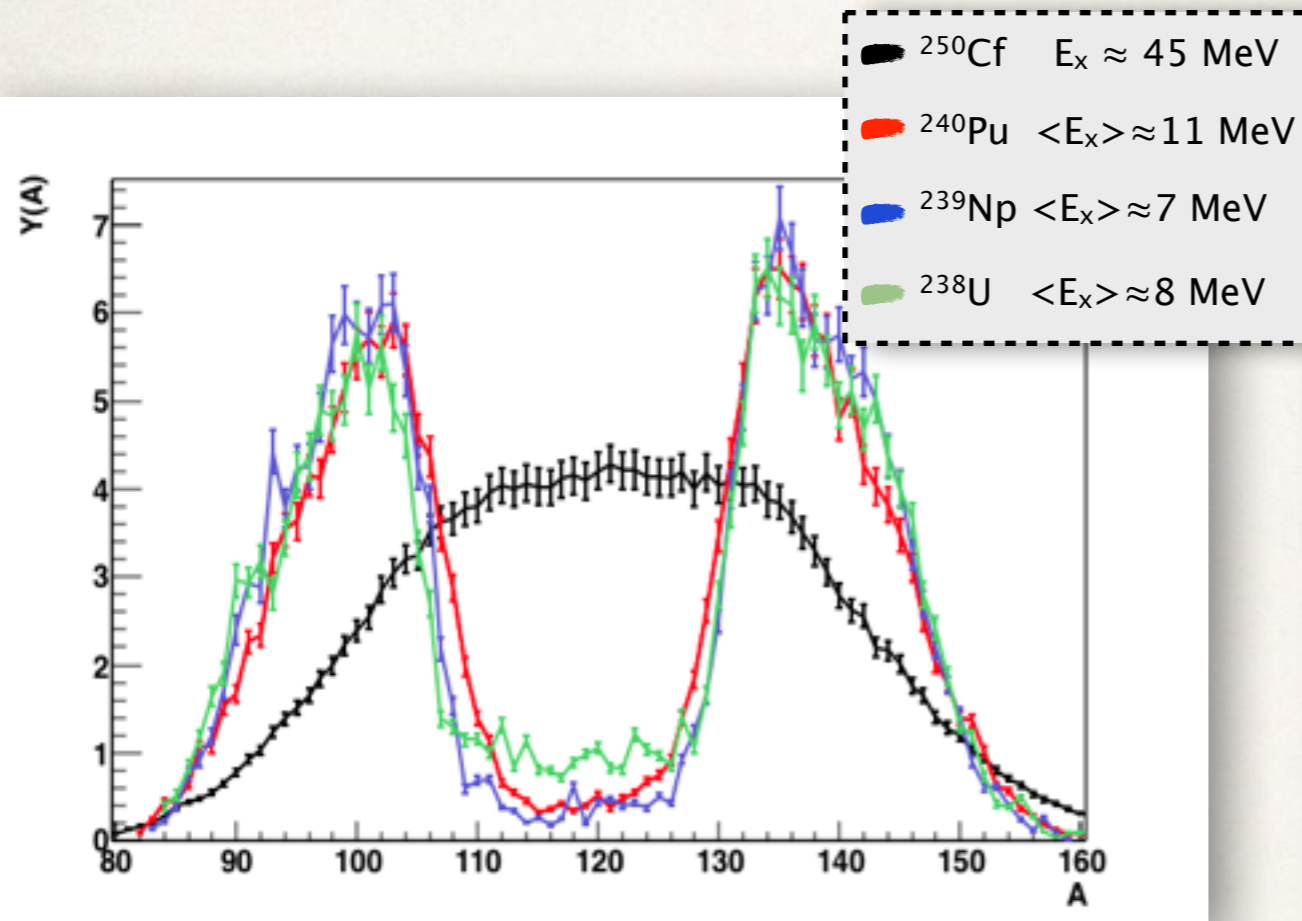
Isotopic Yields in 2 orders of magnitud



A

Fission Yields

Isotopic yields distribution of 4 different fissioning systems, most of them exotic nuclei



New complete measurements, difficult to produce by n-capture

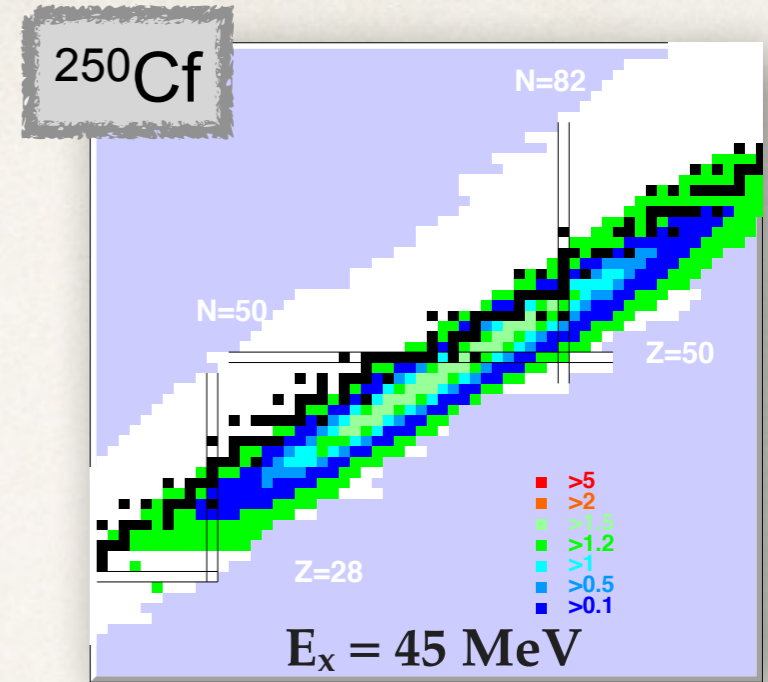
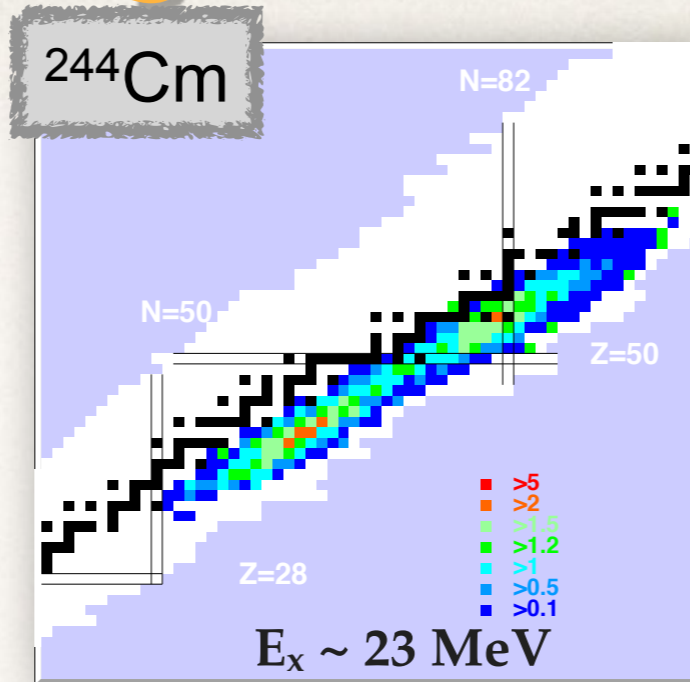
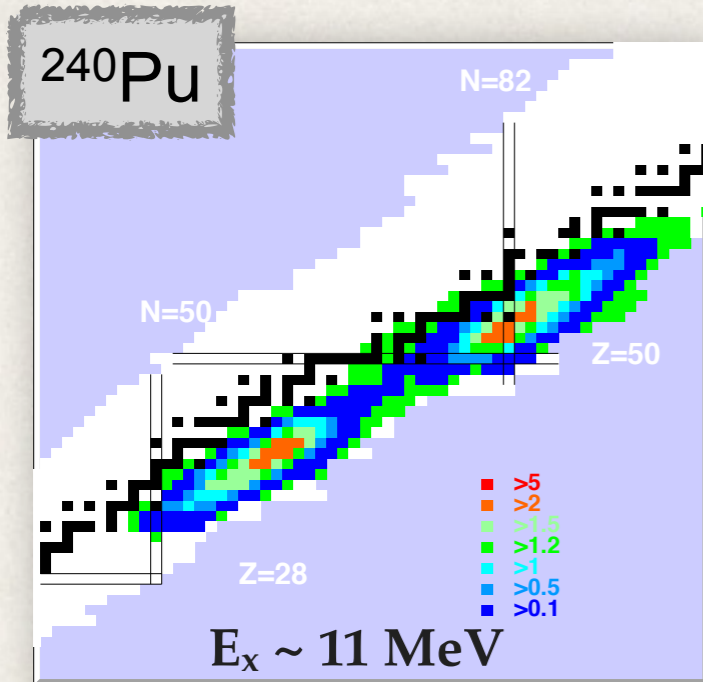
Measurements of fission fragment distributions of ^{239}Np is scarce

$$T_{1/2} (^{238}\text{Np}) = 2.1 \text{ d}$$

The contribution of the symmetric mode disappears for the systems at low excitation energy

The shift in Z of the light fragments reflects the atomic number of the fissioning system

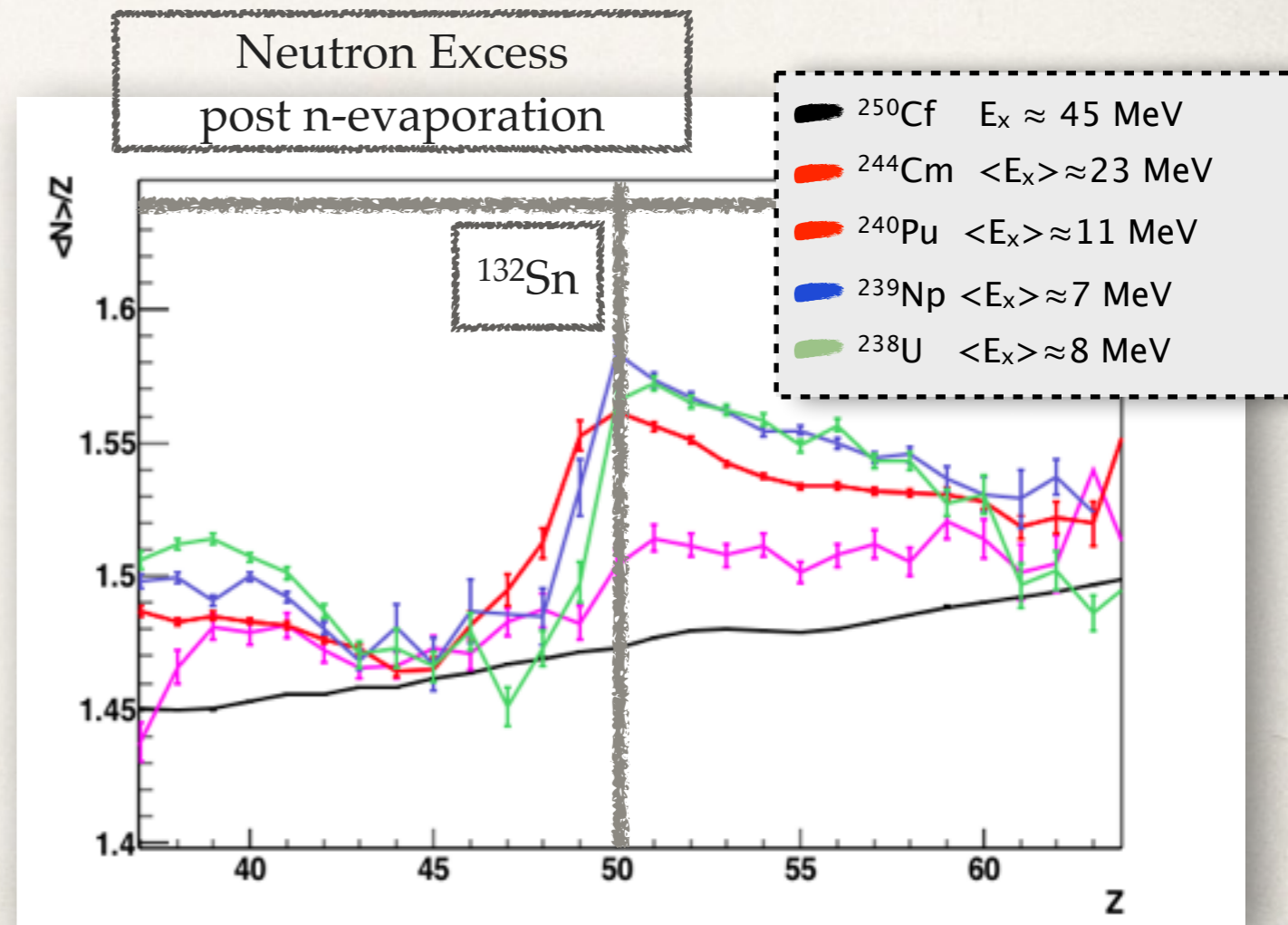
Charge Polarization



Evolution of the polarization with the E_x and the fissioning system

Clear accumulation of N driven by the double magic nucleus ^{132}Sn

Charge Polarization present in all the systems

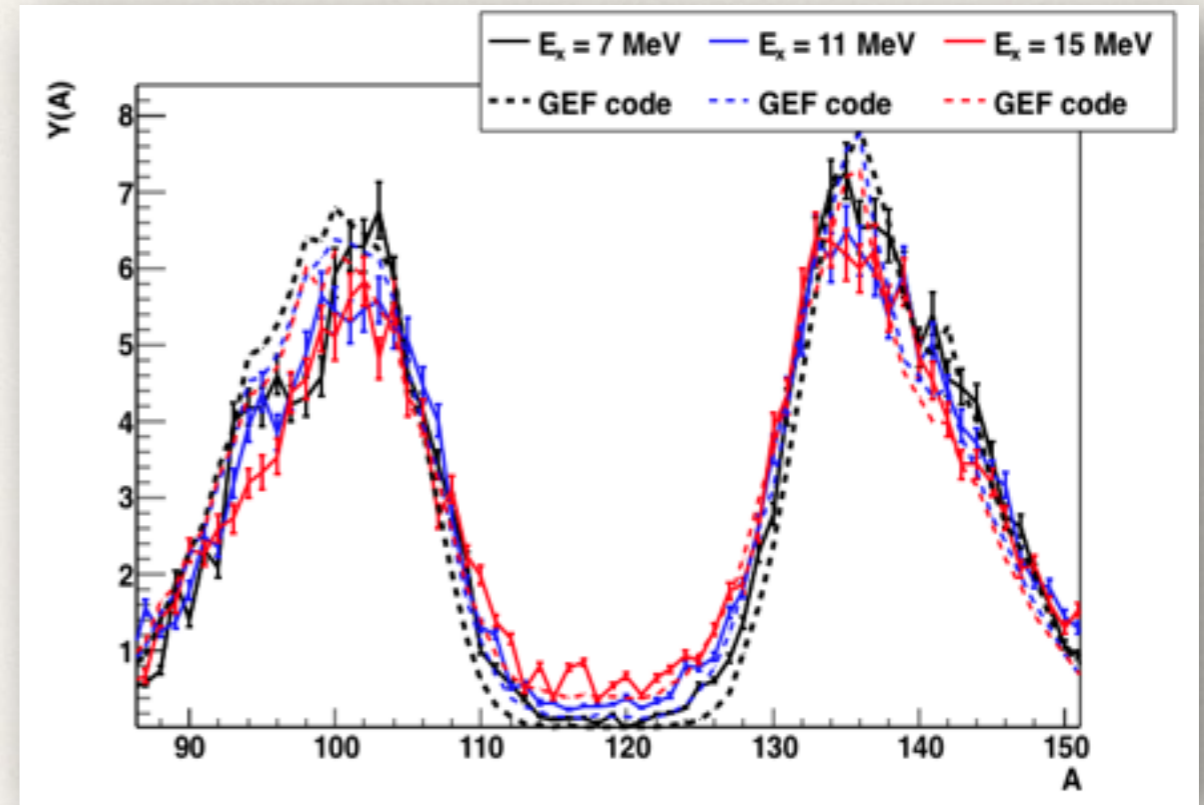
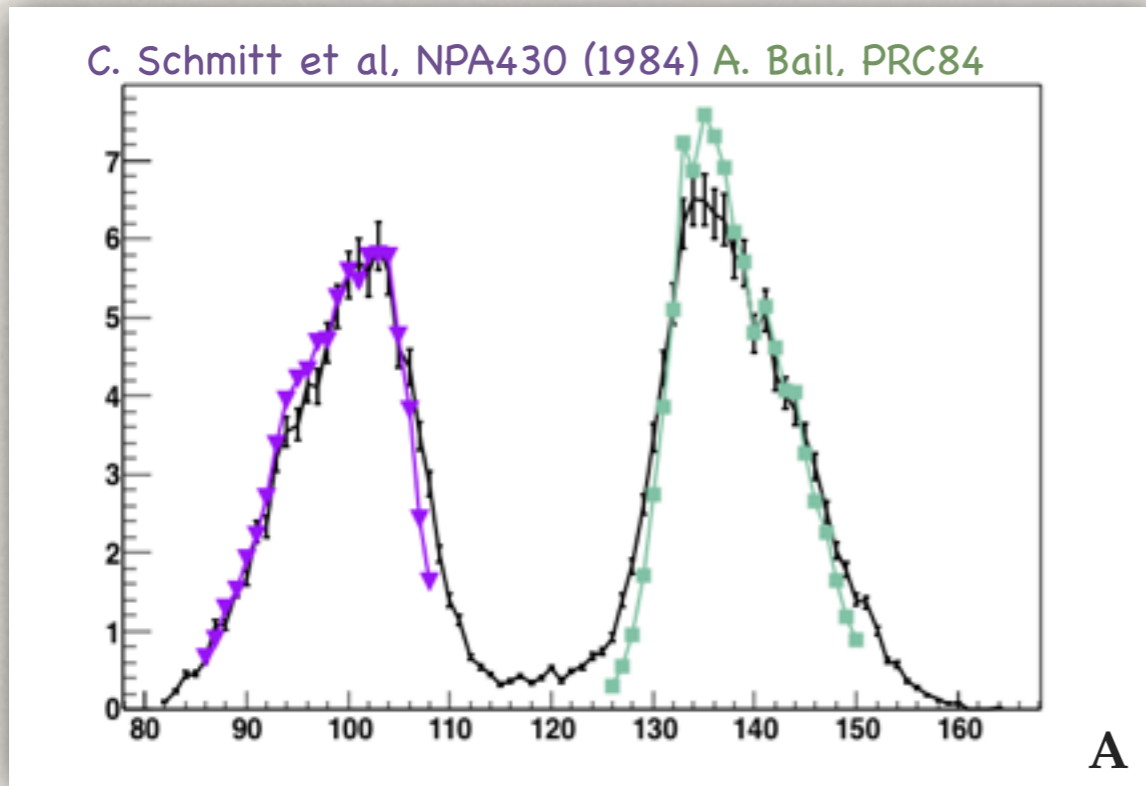


Evolution with Excitation Energy

^{240}Pu

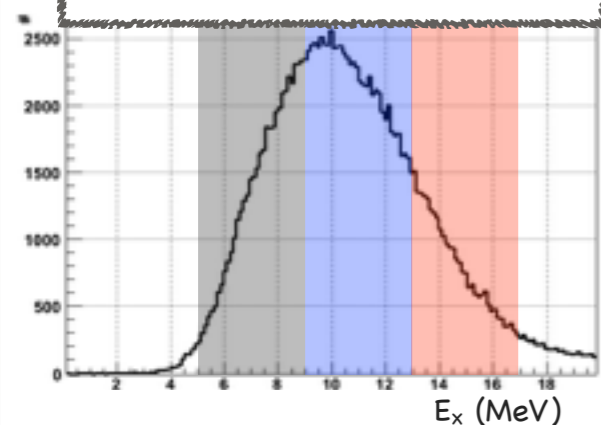
Comparison with previous data

C. Schmitt et al, NPA430 (1984) A. Bail, PRC84

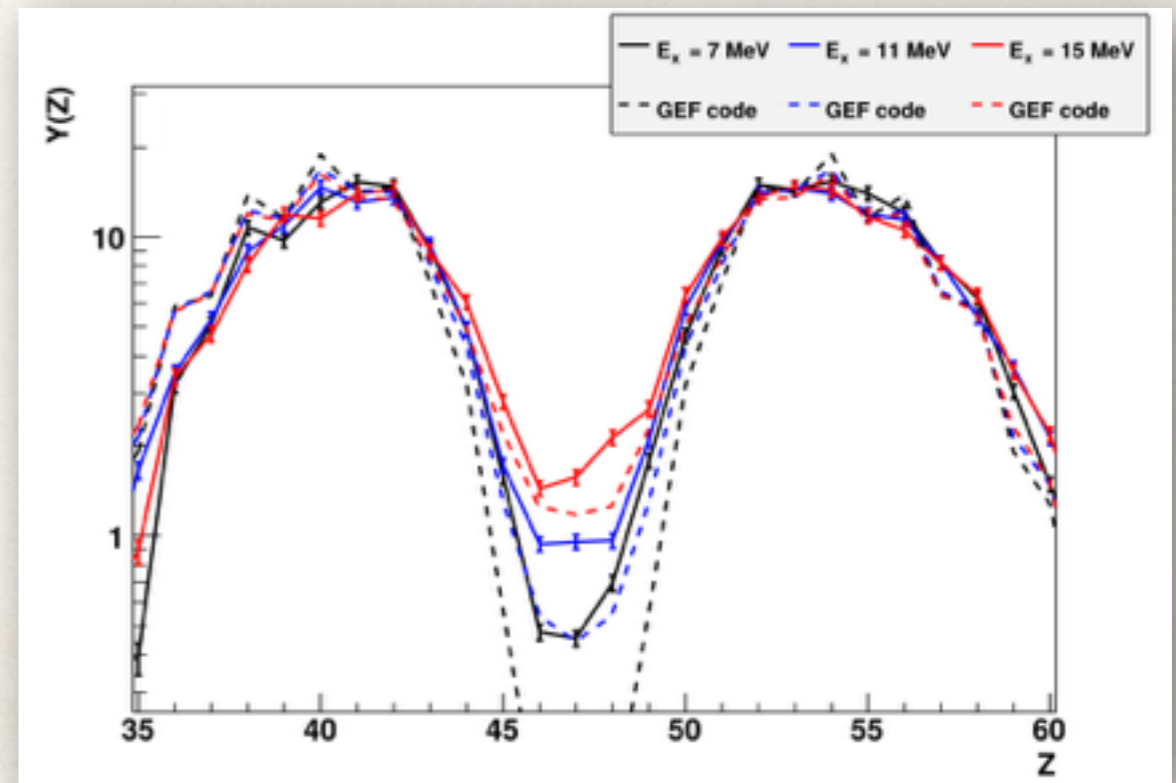


Evolution from asymmetric to symmetric fission by the effect of the excitation energy

$^{238}\text{U}(^{12}\text{C}, ^{10}\text{Be}) ^{240}\text{Pu}$

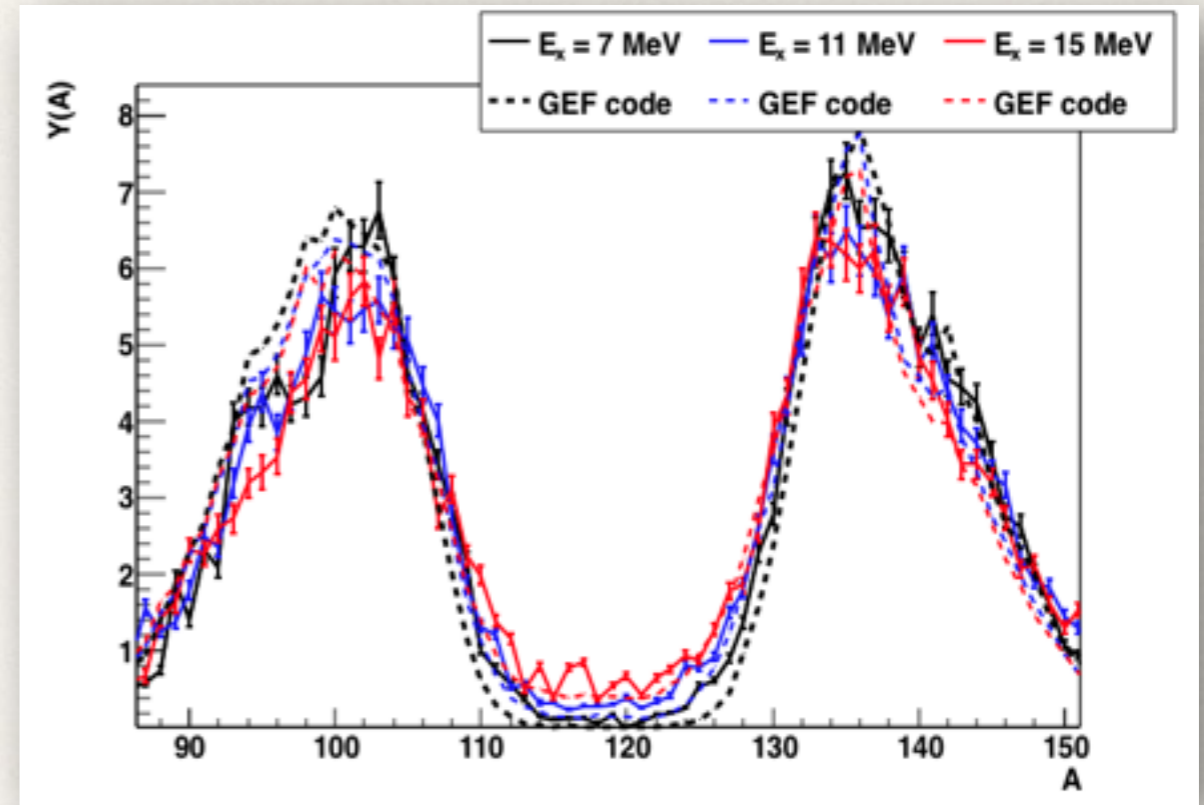
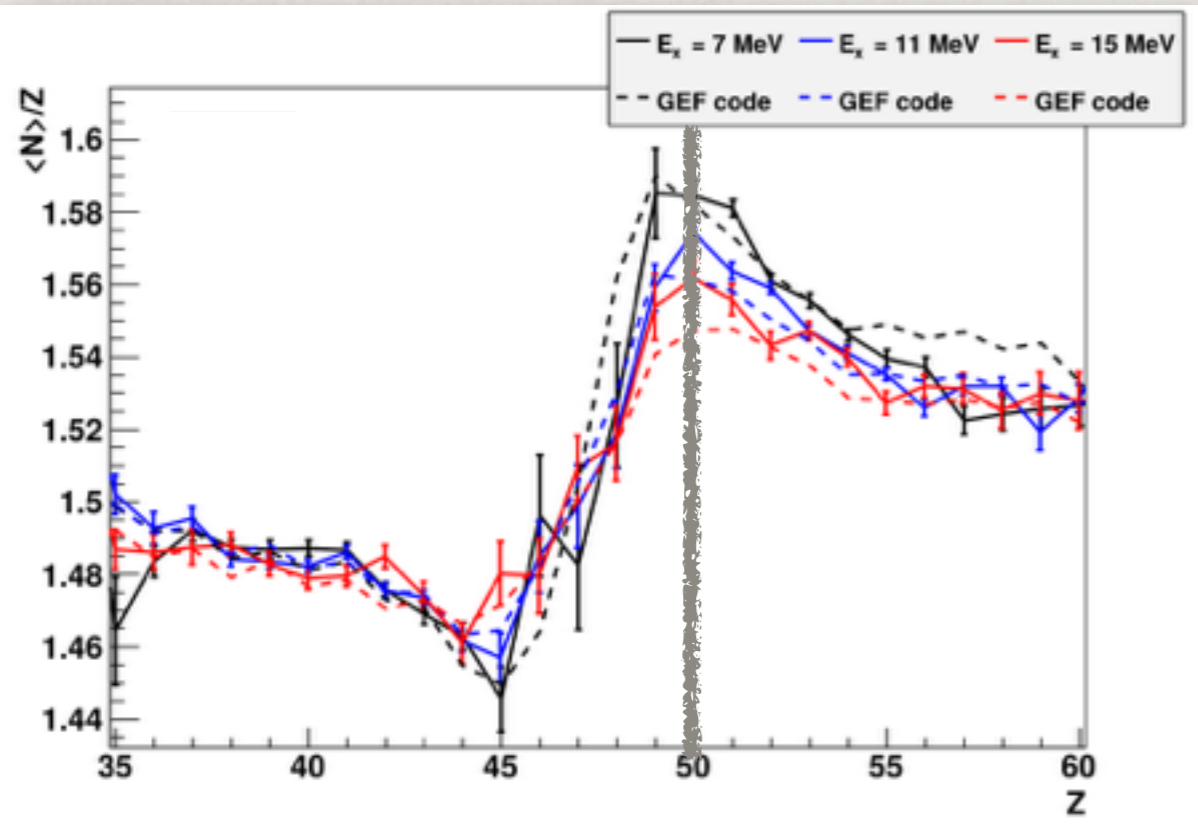


3 different regions of E_x were selected through the transfer reaction reconstruction



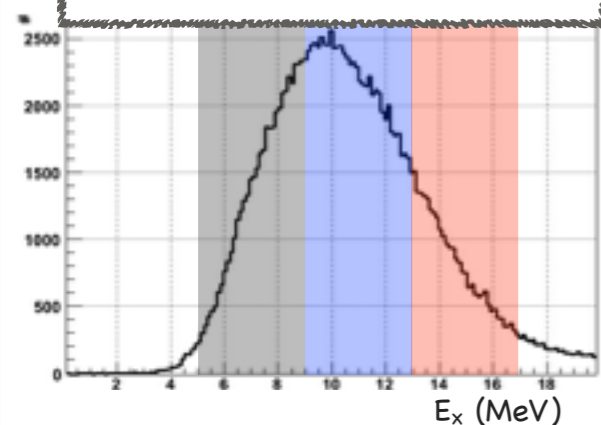
Evolution with Excitation Energy

^{240}Pu

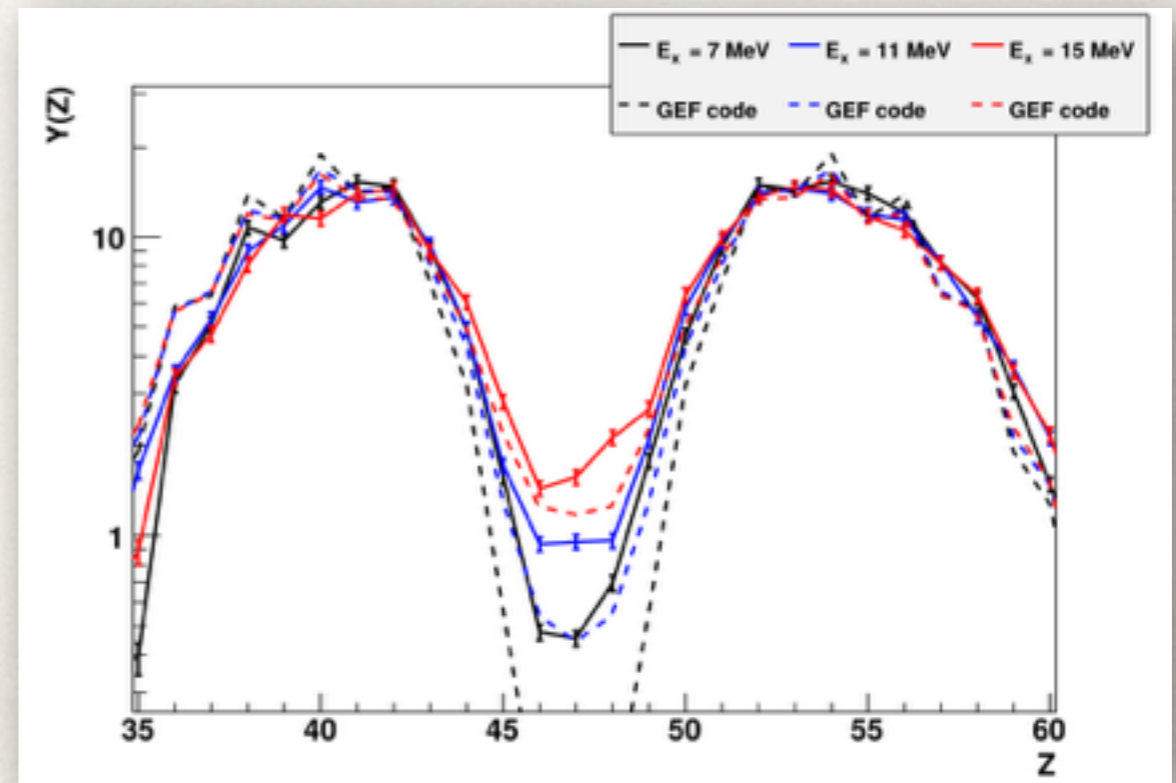


The $\langle N \rangle / Z$ ratio gets reduced around $Z \approx 50$ by increasing E_x , signature of a closed shell which effect is smaller for higher E_x .

$^{238}\text{U}(^{12}\text{C}, ^{10}\text{Be}) ^{240}\text{Pu}$

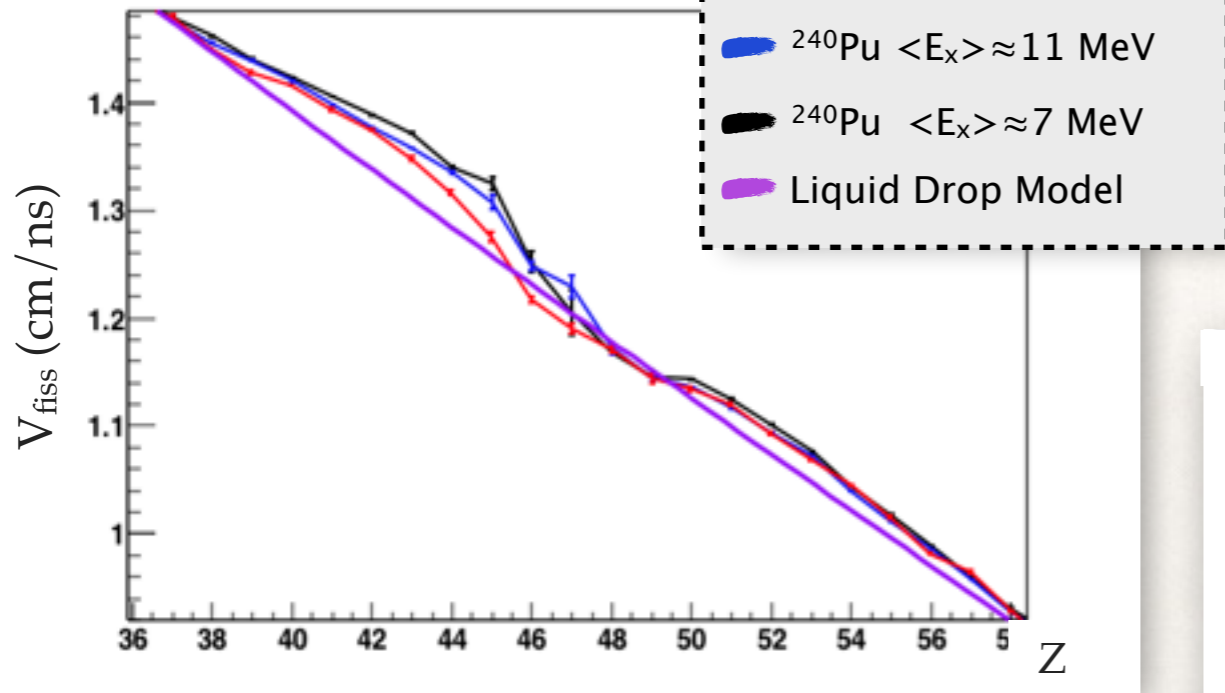


3 different regions of E_x were selected through the transfer reaction reconstruction



Total Kinetic Energy

^{240}Pu

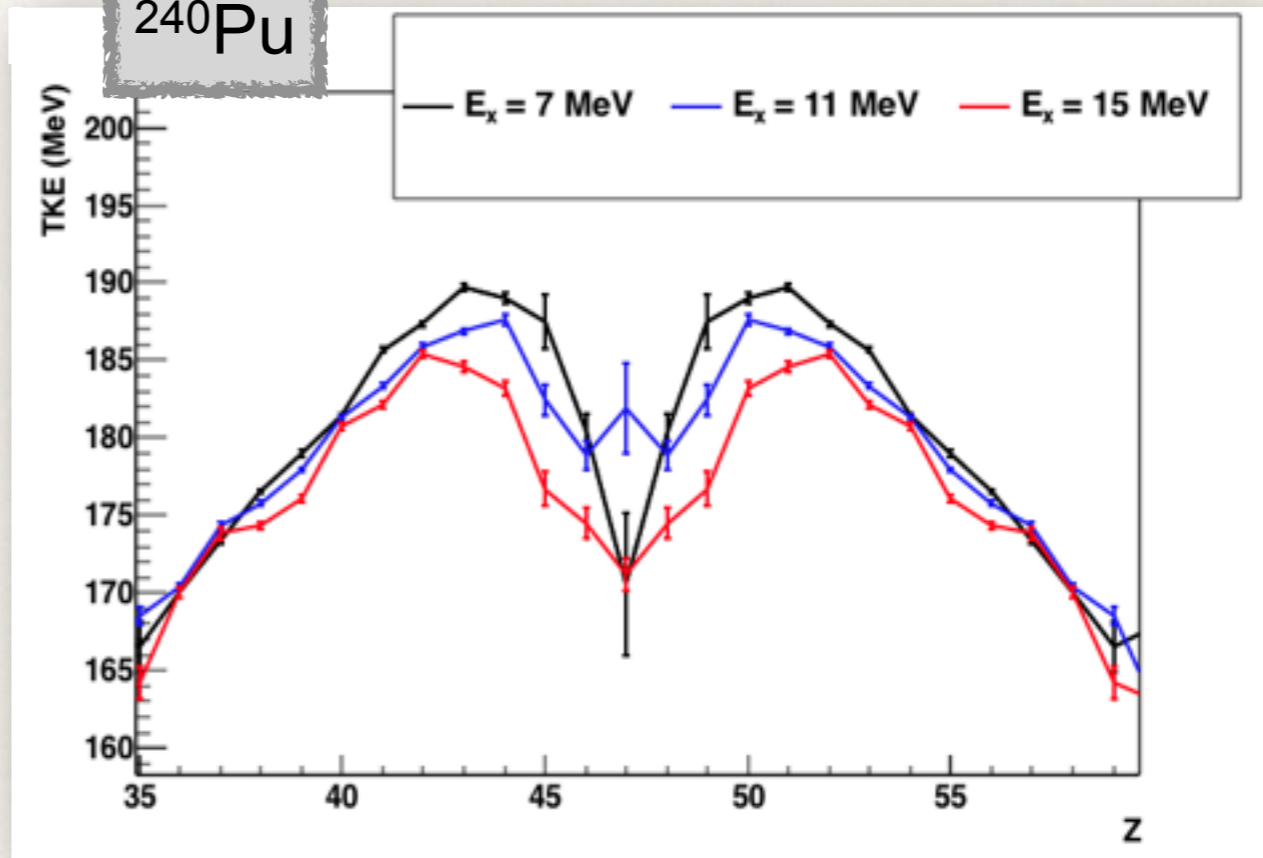


Mean value of the velocity of ff as a function of Z

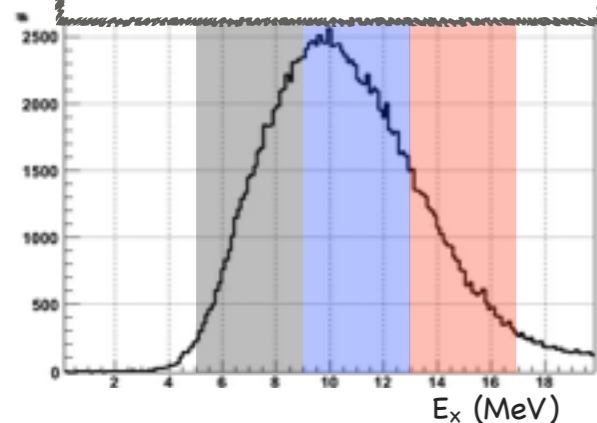
In the asymmetric region, the light fragment is emitted with a higher velocity compared with the LD

$$TKE = u \cdot \langle A \rangle_Z \cdot (\langle \gamma \rangle_Z - 1) + u \cdot \langle A \rangle_{Z_{\text{Act}} - Z} \cdot (\langle \gamma \rangle_{Z_{\text{Act}} - Z} - 1)$$

^{240}Pu



$^{238}\text{U}(^{12}\text{C}, ^{10}\text{Be}) ^{240}\text{Pu}$



TKE values decrease with higher E_x
The distance between both fragments at the scission point is larger with higher E_x

TKE distribution becomes more smooth at higher E_x

Conclusions

Transfer-induced fission in inverse kinematics coupled to the VAMOS spectrometer allowed us to:

Measure the fission of different fissioning systems, most of them exotic nuclei.

Identify the fissioning systems through the reconstruction of transfer reaction channels.

Measure the excitation energy distribution and fission probabilities of each system.

Obtain full isotopic identification of fission fragments using the VAMOS spectrometer.

The effect of closed shells was observed and can be study as a function of the excitation energy in $\langle N \rangle / Z$, TKE, A and Z distributions.

An evolution of the fission fragments from asymmetric to symmetric distributions is observed to follow the excitation energy.

The $\langle N \rangle / Z$ ratio in $Z \approx 50$ is observed to decrease by increasing the excitation energy.